AD-A183 417 MASKING OF LIGHT SCATTERING INFORMATION(U) ARIZONA UNIV 1/1
TUCSON W S BICKEL JUN 87 CRDEC-CR-87089
DAAK11-84-K-0012

UNCLASSIFIED F/G 20/6 NL

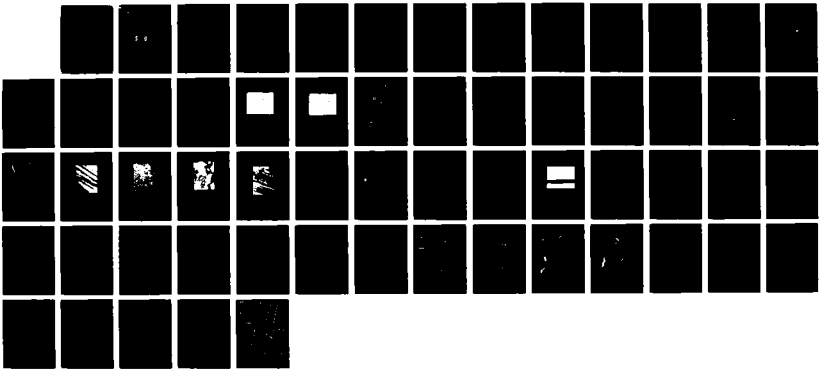

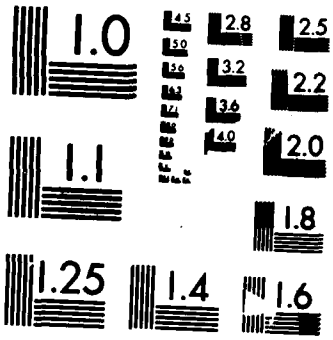

(2)

CHEMICAL RESEARCH, DEVELOPMENT & ENGINEERING CENTER

CRDEC-CR-87089

MASKING OF LIGHT SCATTERING INFORMATION

by William S. Bickel
UNIVERSITY OF ARIZONA
Tucson, AZ 85721

June 1987

U.S. ARMY
ARMAMENT
MUNITIONS
CHEMICAL COMMAND

Aberdeen Proving Ground, Maryland 21010-5423

UNCLASSIFIED
SECURITY CLASSIFICATION OF THIS PAGE

REPORT DOCUMENTATION PAGE

1a. REPORT SECURITY CLASSIFICATION UNCLASSIFIED	1b. RESTRICTIVE MARKINGS
2a. SECURITY CLASSIFICATION AUTHORITY	3 DISTRIBUTION / AVAILABILITY OF REPORT Approved for public release; distribution is unlimited.
2b. DECLASSIFICATION / DOWNGRADING SCHEDULE	
4 PERFORMING ORGANIZATION REPORT NUMBER(S) CRDEC-CR-87089	5. MONITORING ORGANIZATION REPORT NUMBER(S)
6a NAME OF PERFORMING ORGANIZATION University of Arizona 6b. OFFICE SYMBOL (If applicable)	7a. NAME OF MONITORING ORGANIZATION
6c. ADDRESS (City, State, and ZIP Code) Tucson, AZ 85721	7b. ADDRESS (City, State, and ZIP Code)
8a. NAME OF FUNDING / SPONSORING ORGANIZATION CRDEC 8b. OFFICE SYMBOL (If applicable) SMCCR-RSP-B	9. PROCUREMENT INSTRUMENT IDENTIFICATION NUMBER DAAK11-84-K-0012
8c. ADDRESS (City, State, and ZIP Code) Aberdeen Proving Ground, MD 21010-5423	10 SOURCE OF FUNDING NUMBERS PROGRAM ELEMENT NO. / PROJECT NO. / TASK NO. / WORK UNIT ACCESSION NO.

11 TITLE (Include Security Classification)
Masking of Light Scattering Information

12 PERSONAL AUTHOR(S)
Bickel, William S.

13a TYPE OF REPORT	13b. TIME COVERED	14. DATE OF REPORT (Year, Month, Day)	15. PAGE COUNT
Contractor	FROM 84 Sep TO 86 Oct	1987 June	57

16 SUPPLEMENTARY NOTATION
COR: Dr. Jerold Bottiger, SMCCR-RSP-B, (301) 671-2395

17 COSATI CODES			18. SUBJECT TERMS (Continue on reverse if necessary and identify by block number)
FIELD	GROUP	SUB-GROUP	Light Scattering Mueller Matrix Masking
20	06		

19 ABSTRACT (Continue on reverse if necessary and identify by block number)

The author and his students have carried out numerous measurements to explore polarized light scattering from spheres, fibers, and variously prepared surfaces. This report summarizes the results of those investigations and directs the reader to sources in which detailed descriptions of the separate studies have been published.

20 DISTRIBUTION / AVAILABILITY OF ABSTRACT	21. ABSTRACT SECURITY CLASSIFICATION
☒ UNCLASSIFIED/UNLIMITED ☐ SAME AS RPT ☐ DTIC USERS	UNCLASSIFIED

22a NAME OF RESPONSIBLE INDIVIDUAL	22b TELEPHONE (Include Area Code)	22c. OFFICE SYMBOL
Timothy E. Hampton	(301) 671-2914	SMCCR-SPS-T

DD FORM 1473, 84 MAR — 83 APR edition may be used until exhausted. All other editions are obsolete.

SECURITY CLASSIFICATION OF THIS PAGE
UNCLASSIFIED

PREFACE

The work described in this report was authorized under Contract No. DAAK11-84-K-0012. This work was started in September 1984 and completed in October 1986.

The use of trade names or manufacturers' names in this report does not constitute an official endorsement of any commercial products. This report may not be cited for purposes of advertisement.

This document has been approved for release to the public.

ACKNOWLEDGMENTS

The following people have contributed to the work reported in this report:

Vince Iafelice	Grad student
David Abromson	Grad student
Yousif Hashim	Grad student
Wilbur Bailey	Grad student
Tim Carone	Grad student
Sukmock Lee	Grad student
Kaibong Nahm	Grad student
Arleen Watkins	Post Doc
Richard Zito	Research Associate
Martin Goodson	Research Fellow
Joseph Boyer	Visiting Senior Scientist
Gordon Videen	Undergrad
Eric Simms	Undergrad
Andy Spencer	Undergrad
Silvia Tidwell	Undergrad
John Pattison	Undergrad
Kurt Daley	Undergrad
Mark Allen	Undergrad
David Hoar	Undergrad
Brian Watkins	Undergrad
David Graves	Undergrad
Keith Wilson	Professional Internship Program HS student
Wolfgang Gilliar	Visiting Research Fellow

Blank

CONTENTS

LIST OF FIGURES

MASKING OF LIGHT SCATTERING INFORMATION

1. INTRODUCTION

There is one overpowering question concerning light scattering as a diagnostic tool: How good is it? For virtually every other diagnostic technique -- PIXE, neutron activation, ESCA, x-ray flourescence, emmission spectroscopy, nuclear magnetic resonance (NMR), chemistry, etc. -- the range of sensitivity, specificity, resolution, and discrimination is well-known. Many of these techniques produce signals exactly proportional to the "amount" of a specific parameter over many orders of magnitude. In addition, the signals are often traceable through exact theory to fundamental constants. This makes them valuable as diagnostic tools.

When we began this work no such assessment existed for light scattering data. Perfect systems with known optical constants -- refractive index N_1, absorption n_2, and size R -- are special. They generate light scattering signals exactly predicted by theory which often can be inverted to yield n_1, n_2, and R exactly. Studies of such systems can be considered "fundamental research" because all observables can be traced to fundamental optical, electrical, and geometrical constants -- refractive indices, permittivities, dielectric constants and radii. However the motivation for such studies soon "runs out of steam" when there seems no need to further test Maxwell's equations, the speed of light, or pi.

However, as the perfect systems shift gradually to imperfection (irregularity), theory is driven to approximation and finally to complete fantasy where prediction of even the most gross properties of the scatterer and scattering system are suspect. This situation exists because it is experimentally difficult to get a perfect particle system "with a knob on it" to adjust its parameters in an exactly known way while observing its light scattering signal. Nevertheless, this is where the greatest amount of work needs to be done--how to generate exactly known, imperfect, irregular, and complex systems whose properties are still traceable to fundamental constants. These scatterers belong to the real world.

We found a way to solve this problem. Our system is exactly solvable theoretically, attainable experimentally, and complex -- <u>but exactly known</u>. We know that inverted signals do not yield the correct optical constants, but we can find out exactly how close they are. This final report describes some results of our attack on this universally important question.

Our work has shed more light on the validity of light scattering as a diagnostic tool than any theoretical

approximations or extensive experimental studies of uncharacterized, complex irregular particles and particle systems.

Our research dealt with the effects of electromagnetic radiation on small particles (0.01 micron < r < 20 micron) of the order of the wavelength of the incident radiation they scatter (0.4416 and 0.6328 micron).

Our approach used the concept of masking where certain properties of a light scattering signal can be comouflaged, obscured or completely covered up by another. At our disposal are the optical and physical constants n (real refractive index), (absorption) and r (radius) of perfect spheres and fibers. We also investigated scattering signals from irregular particles and mixtures of perfect particles with exactly known concentrations N_1, N_2, ... Ni. In general, our approach has been to slightly perturb perfect experimental systems exactly described by theory while following the perturbation's effect on the light scattering curve. The more gentle perturbations are reversible and produce linear responses to the light scattering curve, while the more severe ones might be irreversible and produce non-linear responses. In all cases we follow the light scattering response as a function of the perturbation strength to relate a signal to a particle property.

Our approach to the problem is summarized with the help of the three particle axes shown in the diagram on the next page. The most obvious place to start a light scattering study is at the origin which represents a Rayleigh particle. This system can be easily solved exactly on the back of the proverbial envelope. As we move out along the "perfect particle" axis, the sphere systems become more complicated. They become larger, hollow, layered, elliptical and finally rod-like (fibers), but still remain exactly, theoretically solvable. This means that electromagnetic theory, coupled with the well-defined geometrical particle boundaries, and optical constants will exactly predict the light scattering signals (all matrix elements S_{ij} as a function of scattering angle). However, even here, the light scattering signals, when inverted, will not always yield the correct optical constants or be unique.

The inability to solve complex systems is not due to the fact that their boundaries are difficult to define mathematically. This is illustrated by the geometrically perfect particles along the y axis. A cube can be defined by one geometrical constant as can a sphere. Yet scattering from a cube cannot be solved exactly in the same way that spheres can. The other geometrical particles along the y axis (pyramids, hexagons, etc.) suffer the same problem. Here theory is not in closed form and if approximations are made the inversion of light scattering data from such particles would not uniquely describe the particle. Note that particles located on the X-Y plane are even more complicated.

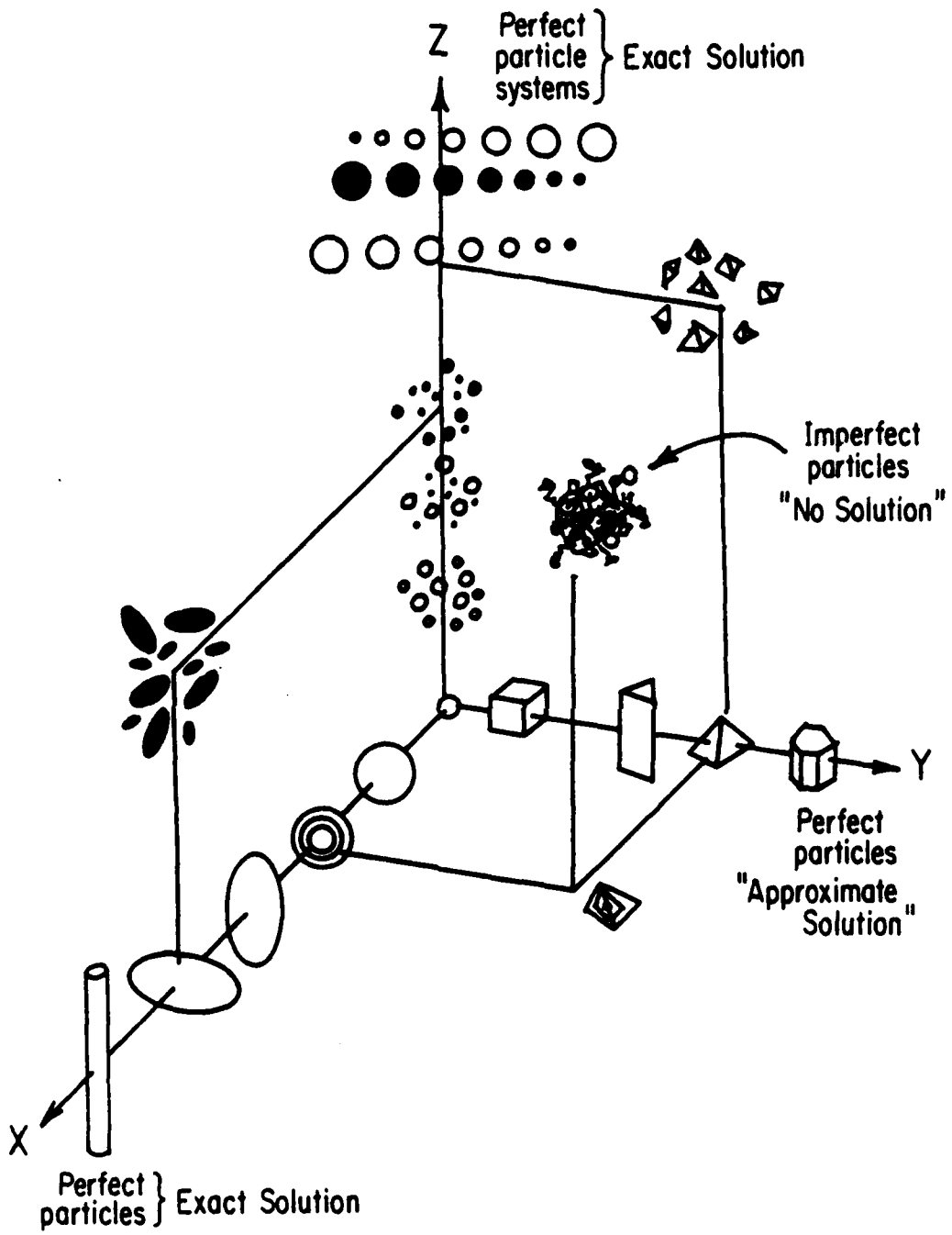
Z
Perfect particle systems
Exact Solution
Imperfect particles "No Solution"
Y
Perfect particles "Approximate Solution"
X
Perfect particles
Exact Solution

In order to get a particle system "with a knob on it," we developed the particle systems indicated along the z axis. They are sphere mixtures which are characterized by three very important and useful properties:

a. they can be solved exactly theoretically

b. they can be created exactly experimentally

c. inversion of the data cannot yield the parameters which describe the system

Since light scattered by a system of spheres is simply the sum of the light scattered by each individual sphere, the light scattering signals from such mixtures are exactly predicted. Only when the mixture is a one-component sphere system will the inversion be unique.

We studied such systems to find how effectively certain particles and particle features could be masked or destroyed by the presence of other particles. We determined which matrix elements S_{ij} are sensitive to masked and perturbed features and which ones best yield the correct optical and physical constants. We also applied various analytical techniques to detect the masked particle or particle feature near detection threshold. Such studies can tell how much light scattering information must be gathered to get an accurate description of the scatterers--which matrix elements and what -range contain the most useful information.

Our first studies dealt with perfect spheres and fibers for which the errors and uncertainties could be related to fundamental constants. Our later work dealt with the more complex problem of sphere mixtures and finally irregular particles and irregular particle systems. Although the conclusions we draw are often very system-dependent, the techniques we developed can be used to directly assess the accuracy of the optical and physical constants obtained from light scattering data from many real-life systems. Since virtually all light scattering (environmental, biological, astronomical, physical, industrial, etc.) is from non-perfect systems, this approach has special significance, and the results have special value for the analysis of real and natural scatterers.

Our most recent studies dealt with surface scattering. In particular we studied perfect (ideal) reflecting surfaces, slightly degraded surfaces and perfect surfaces on which we put an exactly known geometrical line of width w and hight h with w, h . All 16 matrix elements were studied for this system and compared with diffraction from a single fiber and a single slit. Exact theory for such systems is essentially nonexistent. We also studied the scattering from a perfect circular cross sectional cylinder lying on a perfect reflector. No theory exists for this system either. Both the line and the fiber can

be considered to be cylinder on a surface are considered to be exactly characterized "defects" on a surface. Even though the cylindrical case lends itself to exact theoretical solution, as yet no complete theory exists. We then extended our work to liquid coated surfaces where the S_{ij} were measured as a function of liquid thickness which changed in time due to evaporation. All S_{ij} show peculiar behavior not explainable simply in terms of interference effects. We then investigated porous surfaces where liquids could diffuse beneath the surface. This work is still under way.

Finally we theoretically obtained the exact scattering solution of two parallel fibers, tilted at arbitrary angle and made of arbitrary composition. All results appear as matrix elements and demonstrate the rich detail that accompanies the subtle interference effects between two fibers illuminated with a plane em wave.

This final report will list all publications reporting work done under this contract along with a brief outline of the main results of each paper.

2. RESULTS

In this section we list all recent publications, submittals for publications and presentations that resulted from the work done on this project. Each paper is followed by a short description of the main points of the paper. We point out that the last two year's work has contributed to:

3 papers published
6 papers accepted
2 papers submitted
2 Ph.D theses
2 MS. theses
3 presentations
5 papers in preparation

2.1) W. S. Bickel and W. M. Bailey, "Stokes Vectors, Mueller Matrices and Polarized Scattered Light," Am. J. Phys., Vol. 53, May 1985, 468 - 478.

The complete characterization of scattered light is described in the context of Stokes vectors and Mueller matrices which highly motivates the measuring procedures. The most general form of the scattering matrix coupled with polarizers and quarter wave plates elegantly demonstrates the physical relationship among the matrix elements and polarization measurements.

2.2) A. J. Watkins and W. S. Bickel, "A Study of the Kirlian

Defect," The Skeptical Inquirer, Vol. X, No. 3, Spring 1986.

A study of the Kirlian effect on living and nonliving surfaces shows that the aura shape depends on many factors that need careful control. The aura itself is nothing more than the contact photograph of the air plasma that surrounds the boundary of the item being studied. The aura can be used to detect defects that lie under a surface which would be invisible to optical detection.

2.3) R. R. Zito and W. S. Bickel, "Light Scattering from Twisted Metal Cylinders," App. Optics, Vol. 25, 1986.

The twisting of polished cylinders beyond the elastic limit results in the formation of surface cracks in the smooth surface. These surface cracks scatter light in a characteristic way. For small plastic deformations, the light scattering properties of the surface depend linearly on the permanent twist angle. Therefore, light scattering may be used as a kind of strain gauge.

2.4) W. Gilliar, W. S. Bickel, G. Videen, and D. Hoar, "Light Scattering from Fibers: An Extension of a Single Slit Diffraction Experiment," Am. J. Phys., 1986. (Accepted)

The similarities and differences between diffraction from single slits and scattering from single fibers can be dramatically demonstrated by some simple experiments. Geometrical properties such as fiber size, cross-section, tilt, and non-uniformity all contribute to the intricate detail of the diffraction pattern. An examination of the role of the complex refractive index, polarized light, and geometrical effects in scattering phenomena will contribute to a deeper understanding of the interaction of light with small apertures and particles.

2.5) W. S. Bickel, A. J. Watkins and G. Videen, "The Light Scattering Mueller Matrix Elements for Rayleigh, Rayleigh-Gans and Mie Spheres," Am. J. Phys., 1986. (Accepted)

The four nonzero light-scattering matrix element curves for spheres near the Rayleigh and Rayleigh-Gans limit are compared as the respective limits are approached by a large, high-refractive-index Mie sphere.

2.6) G. Videen and W. S. Bickel, "Light Scattering from Geometrically Perturbed Quartz Fibers," App. Optics, 1986. (Accepted)

Light scattered from a "perfect" cylindrical quartz fiber was studied as a function of fiber rotation, bend, bend and

rotation, and tilt. These pure geometrical manipulations are basic and easily controlled perturbations that affect both the total intensity and geometrical distribution of the scattered light. The scattering patterns from these perfect fibers are more complex than first suspected.

2.7) V. J. Iafelice and W. S. Bickel, "Polarized Light Scattering Matrix Elements for Select Perfect and Perturbed Optical Surfaces," App. Optics, 1986. (Accepted)

The angular distribution of scattered light depends on the electromagnetic properties (refractive index, absorptivity), the geometrical properties (size, shape, and distribution) of the scatterer(s), as well as the polarization and illumination angle of the incident light. To study the total information content, we measured the entire experimental 16-element Mueller scattering matrix for a smooth reflecting aluminum surface illuminated with = 4416A light at various angles of incidence, . In comparison, we also measured the scattering matrix for a degraded smooth reflecting aluminum surface This paper discusses the experimental procedure and compares the scattering results obtained from these two types of surfaces. The following figures 1 - 6 taken from this paper, show the data and results of these experiments.

2.8) W. S. Bickel, V. Iafelice, and R. R. Zito, "Polarized Light Scattering from Metal Surfaces," J. App. Physics, 1986. (Accepted)

The stretching and bending of polished and industrial-grade metallurgical surfaces changes the appearance of the specimen's surface. The changes in surface structure can be detected in the polarized light scattered from the surface cracks and other defects, which act as scattering centers. In order to interpret light scattering signals from complex surfaces, we first examine the nature of light scattered from a perfect mirror surface, a degraded mirror, a line on a mirror, a randomly sanded surface, and finally the industrial grade metal surfaces damaged by stretching and bending. The following figures 7 - 18, taken from this paper, show the data and results of these experiments.

2.9) V. Iafelice and W. S. Bickel, "Polarized Light Scattering Matrix Elements for Micron-sized Rectangular Aluminum Lines and Reflecting Optical Surfaces," 1986. (Accepted)

The entire 16-element Mueller scattering matrix has been experimentally determined for several small rectangular cross sectioned aluminum lines whose known dimensions are of the order of the incident light (wavelength = 4416A). Each line was fabricated on top of a smooth reflecting aluminum surface using electron beam lithography techniques. The Mueller

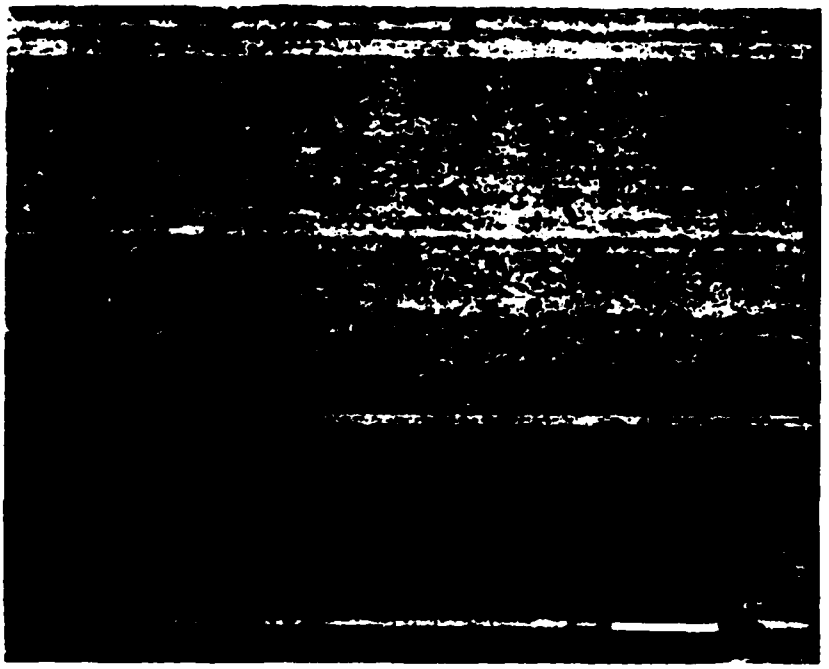

Figure 1. The Perfect Mirror Surface (PMS) Magnified One Thousand Times. (Bar line = 10 microns.)

Figure 2. The Degraded Mirror Surface (DMS) Magnified One Thousand Times. (Bar line = 10 microns.)

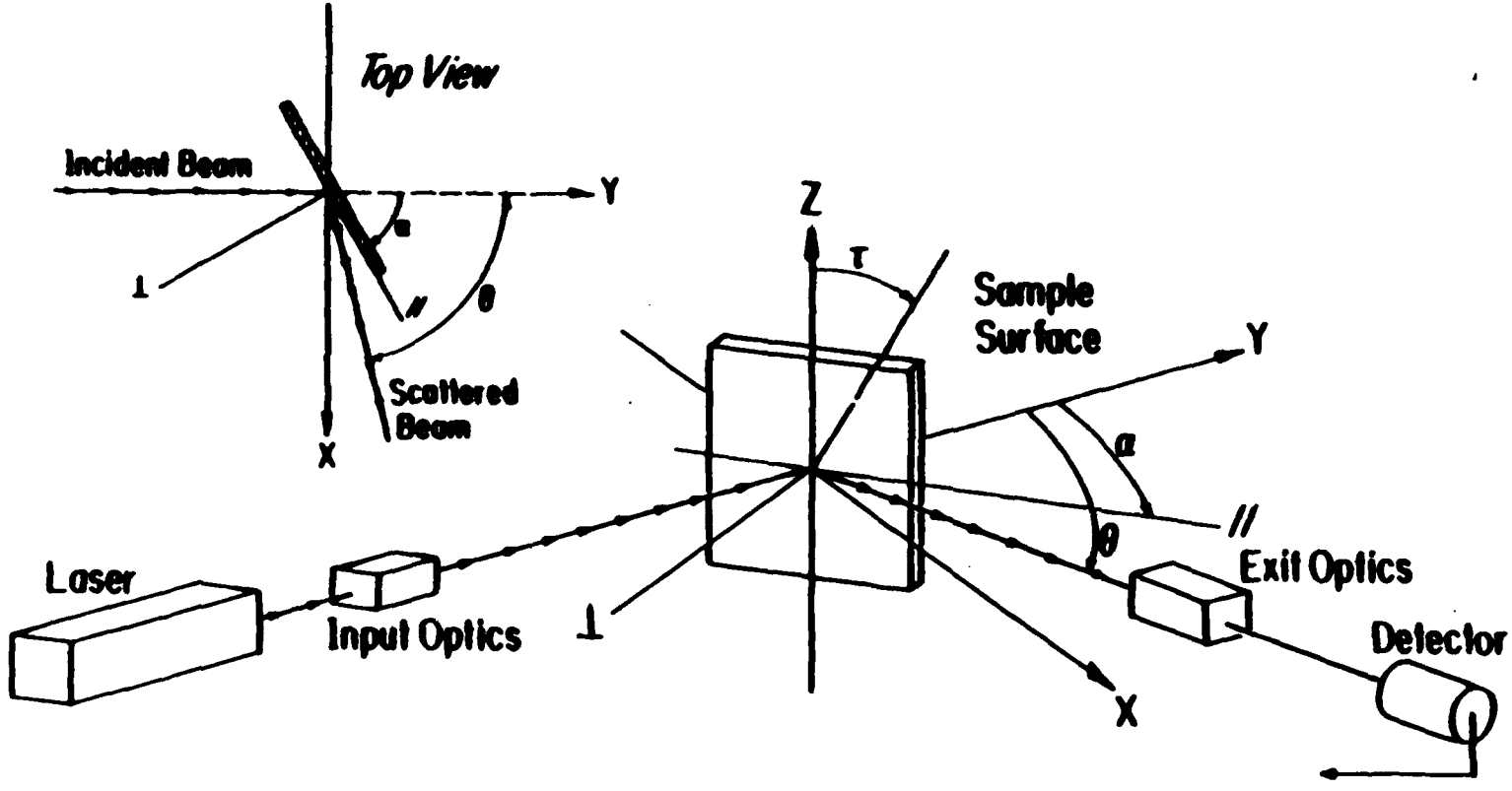

Figure 3 Relationship Between the Various Sample Orientation Parameters.

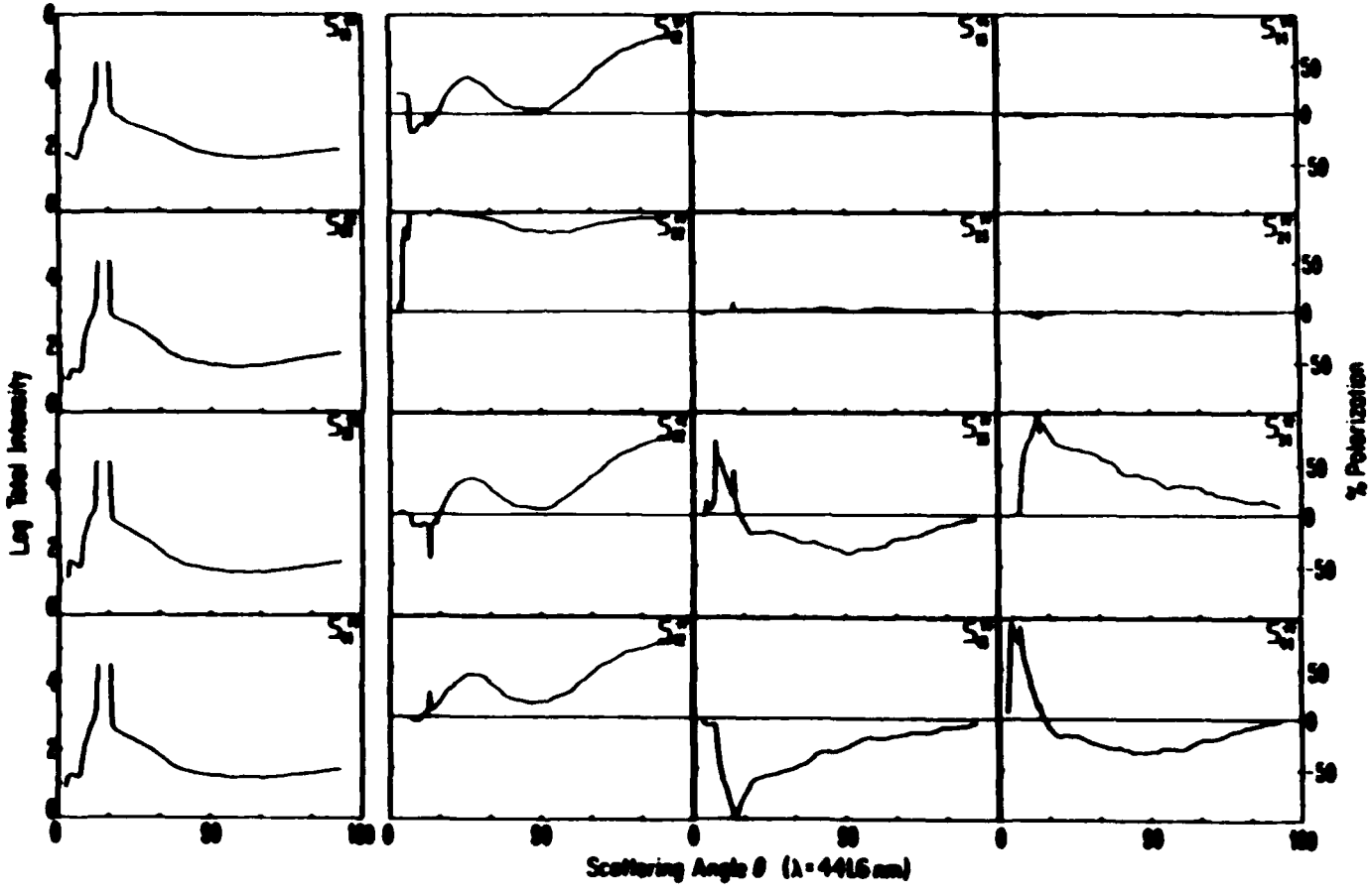

Figure 4. The Entire Mueller Matrix S^{*}_{ij} (θ), for the Perfect Mirror Surface (PMS) Illuminated at Grazing Incidence ($\alpha = 11^{\circ}$).

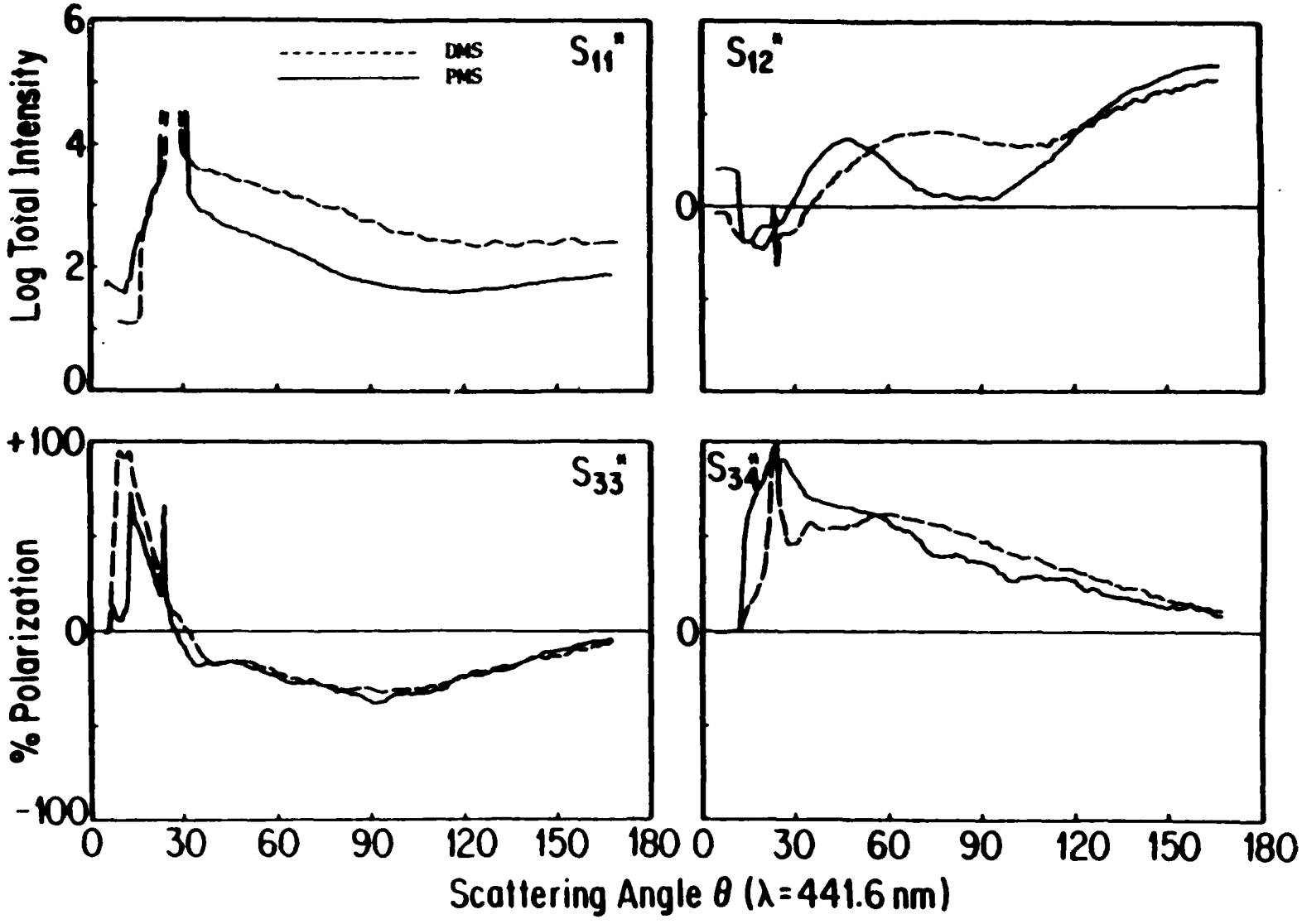

Figure 5. Four Matrix Element Curves for the Perfect Mirror Surface (Solid Line) and the Degraded Mirror Surface (Dashed Line) Illuminated at Grazing Incidence ($\alpha = 11^{\circ}$).

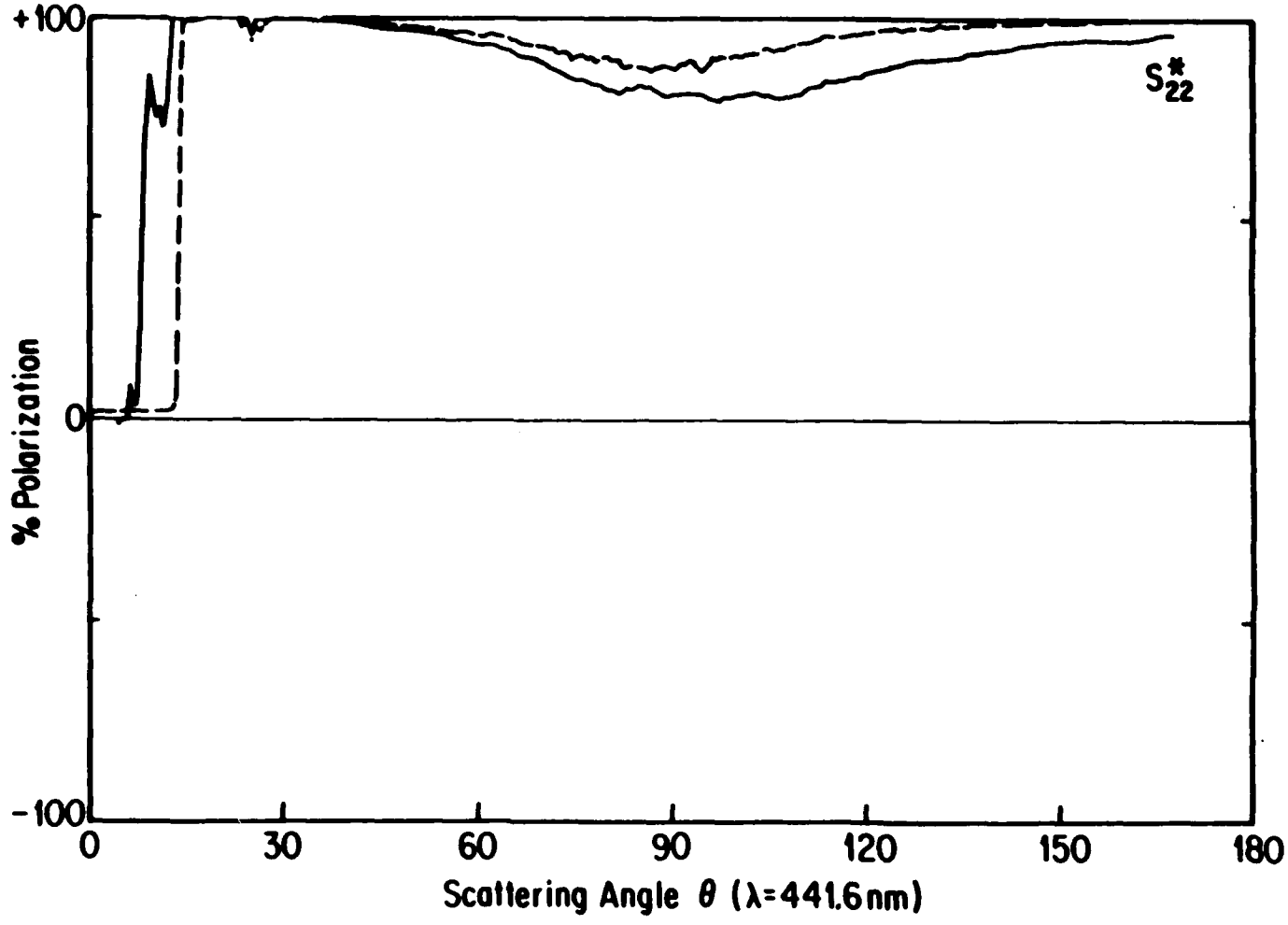

Figure 6. The S^*_{22} Matrix Element Curves for the Perfect Mirror Surface (Solid Line) and the Degraded Mirror Surface (Dashed Line) Illuminated at Grazing Incidence ($\alpha = 11^\circ$).

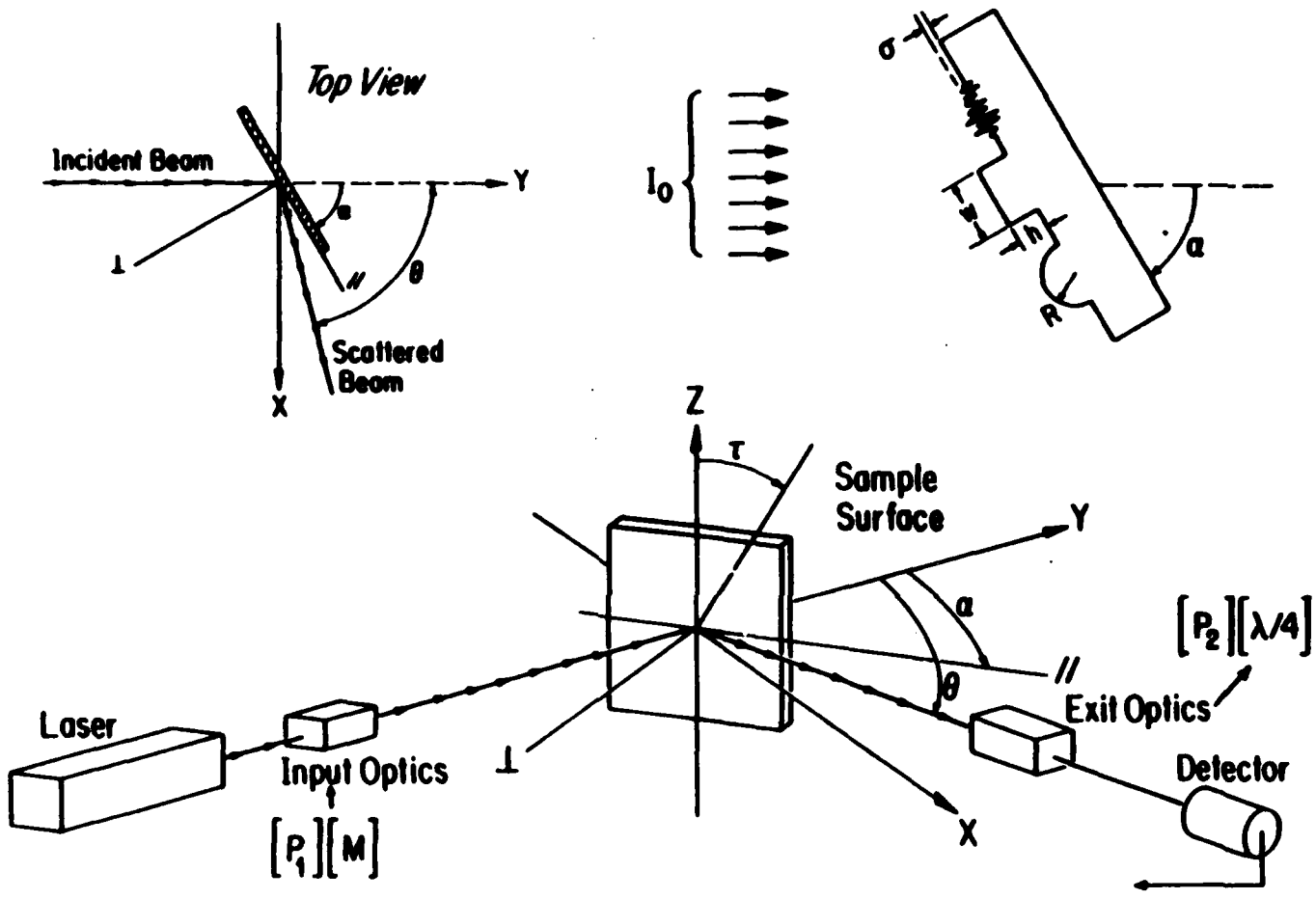

Figure 7. Relationship Between the Various Sample Orientation Parameters. (Top Right) Idealized Surface Geometries Showing Surface Microroughness (σ, not to scale), and the Perfect Aluminum Line on a Perfect Mirror Surface.

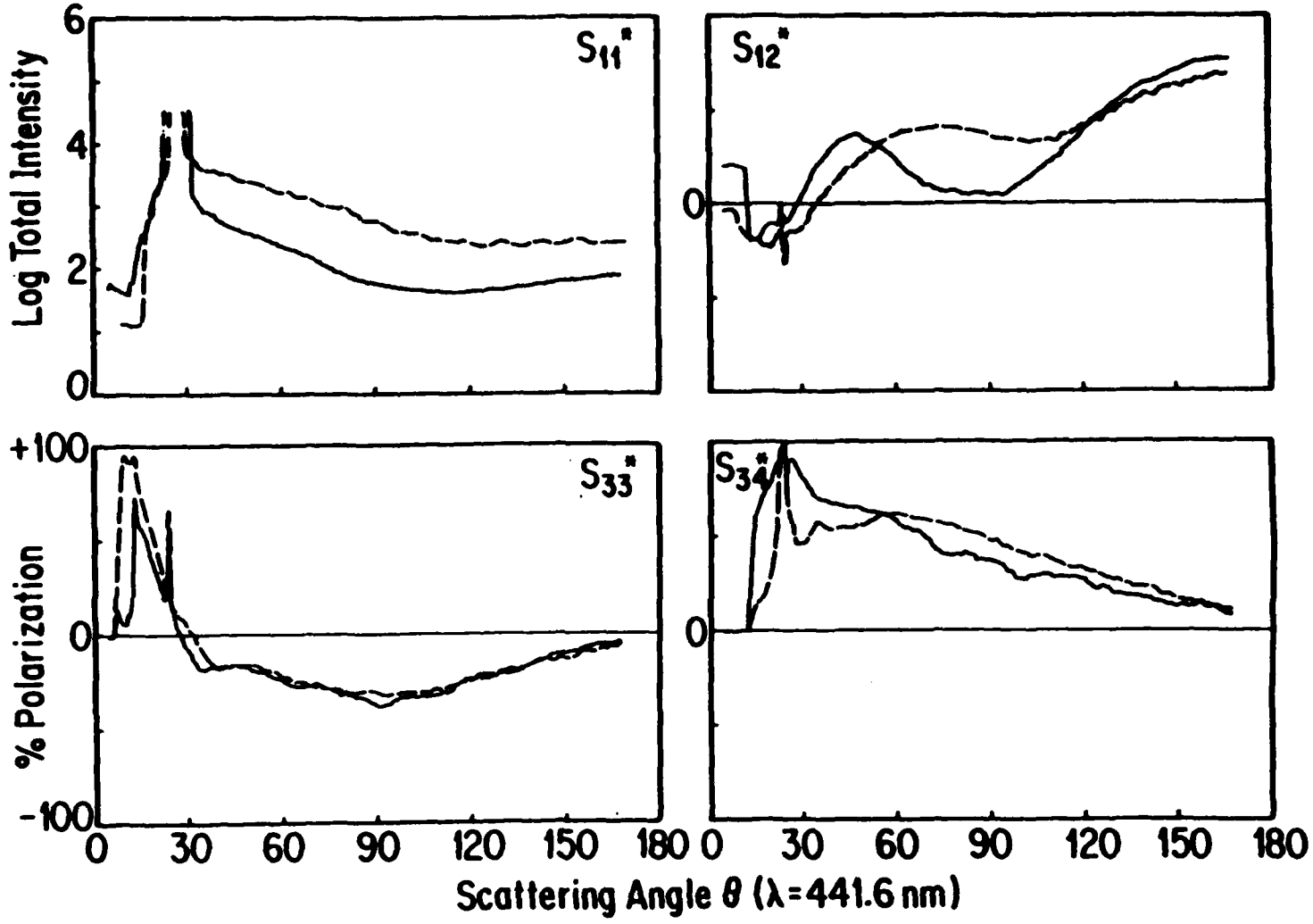

Figure 8. Four Matrix Element Curves for the Perfect Mirror Surface (Solid Line) and the Degraded Mirror Surface (Dashed Line) Illuminated at Near Grazing Incidence ($\alpha = 15^{\circ}$).

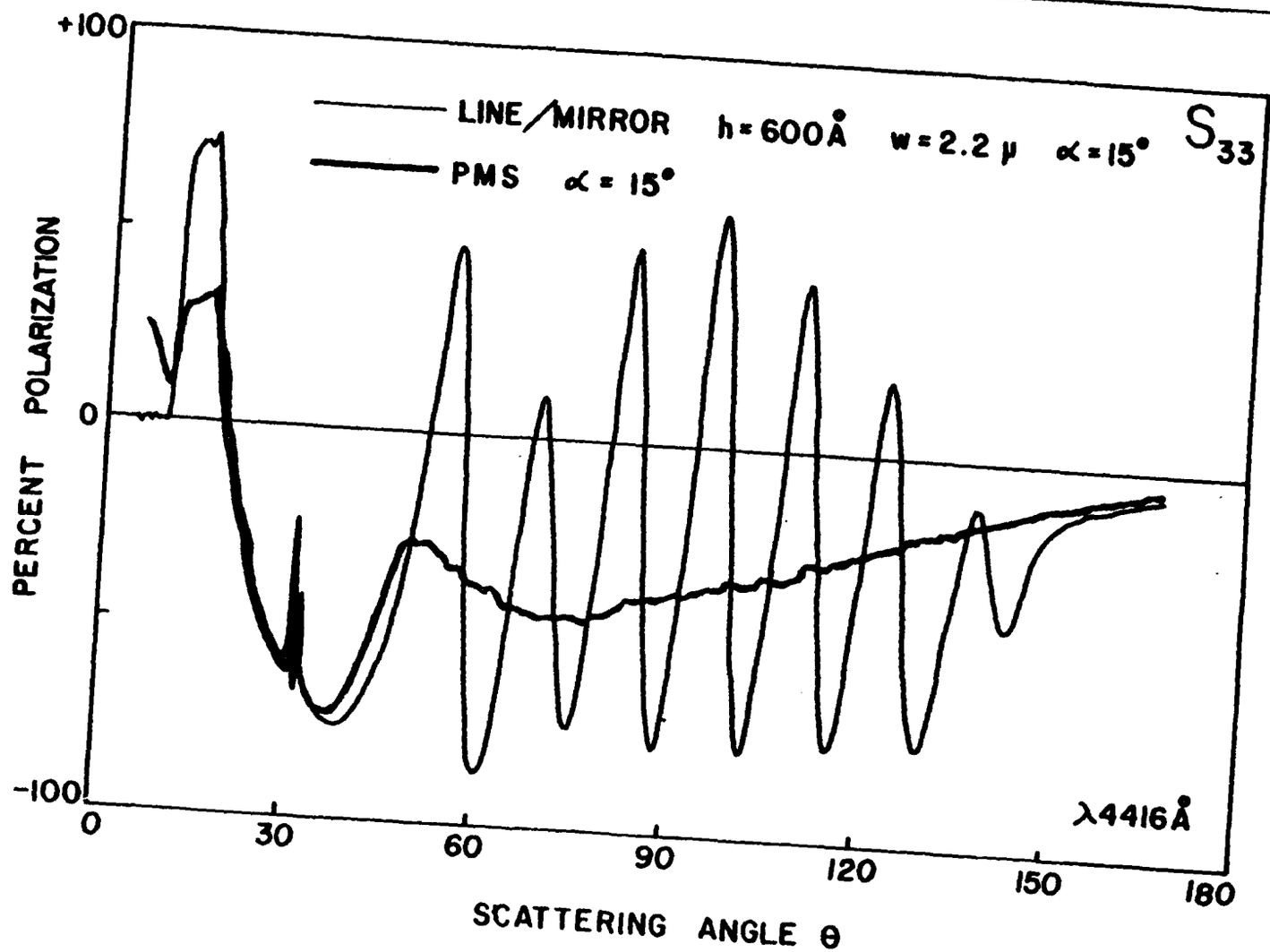

Figure 9. The S_{33} Matrix Element for a line/mirror sample ($h = 600$ Å, $w = 2.2$ m) and for the PMS, Both at Near Grazing Incidence ($\alpha = 15^{\circ}$).

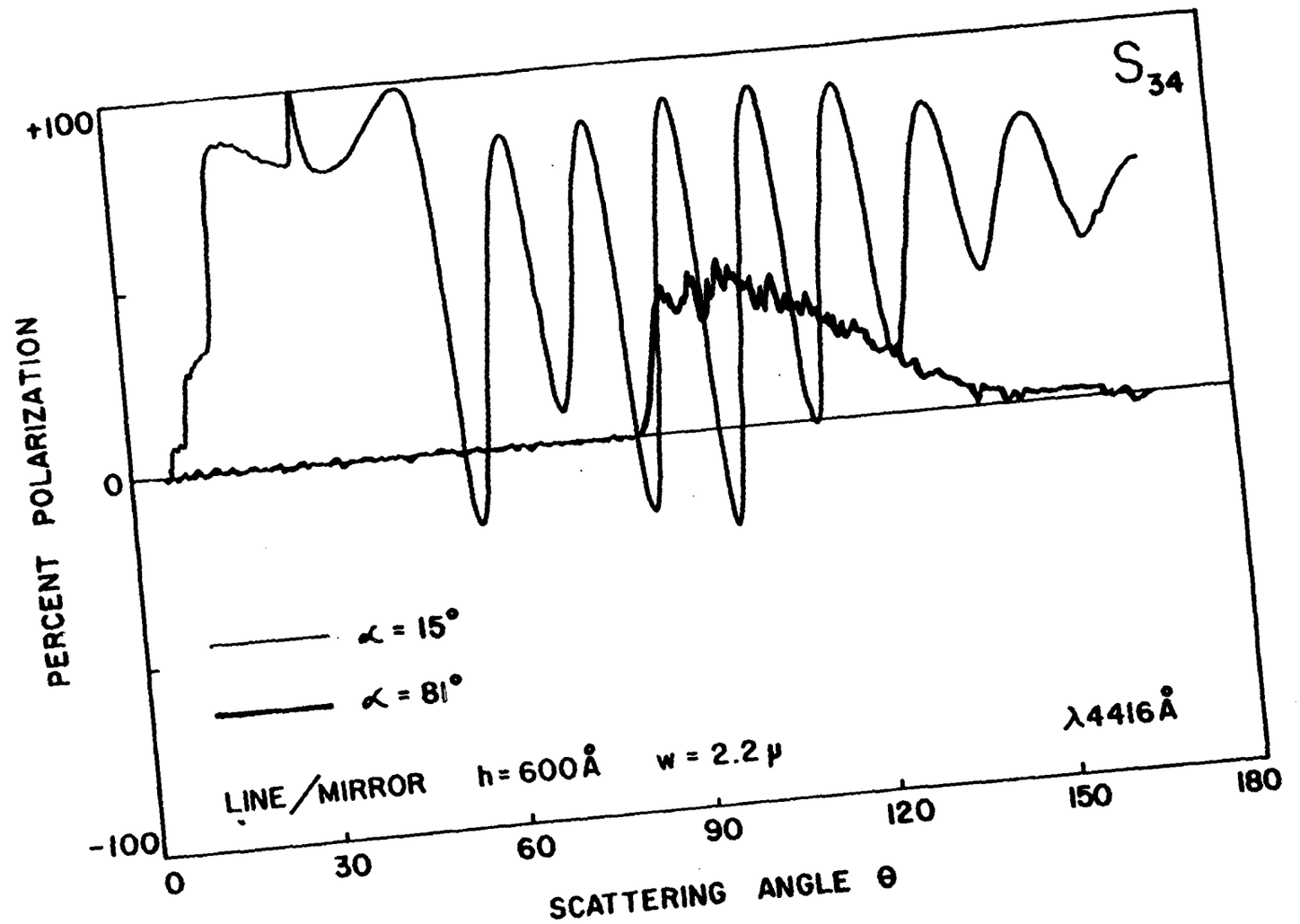

Figure 10. The S_{34} Matrix Element for a Line/Mirror Sample ($h = 600$ Å, $w = 2.2$ μm) Illuminated at Near Grazing Incidence ($\alpha = 15^{\circ}$) and at Near Normal Incidence ($\alpha = 81^{\circ}$).

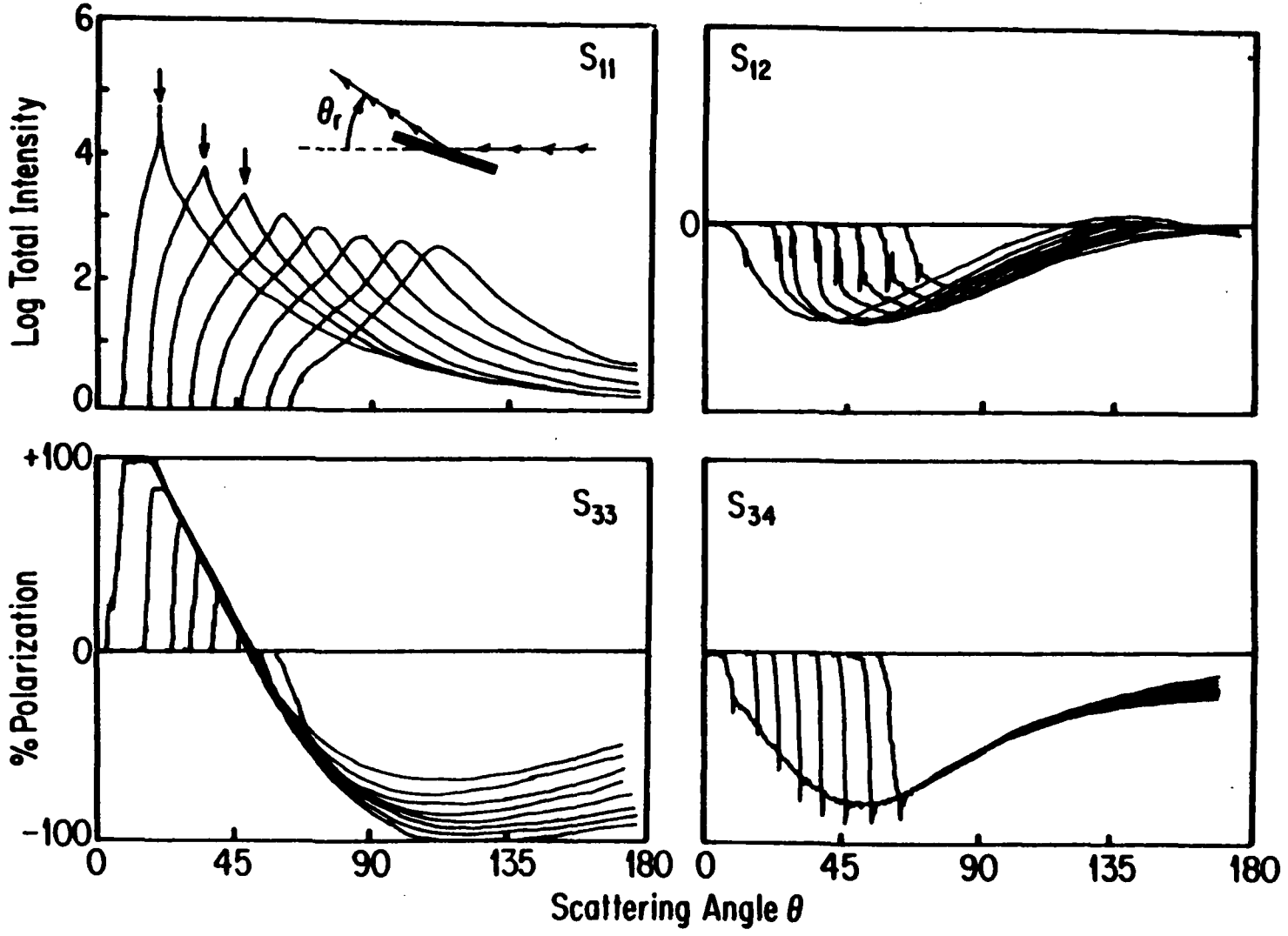

Figure 11. Four Matrix Elements for a Randomly Sanded Brass Surface Illuminated at Various Angles of Incidence, $\alpha = \theta_r/2$.

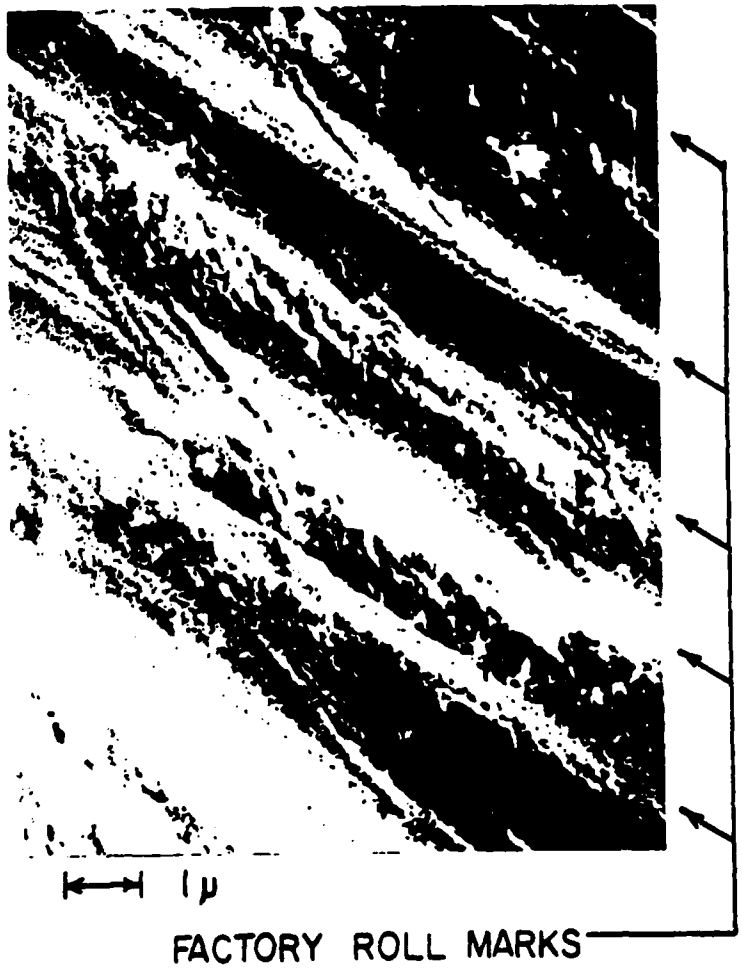

Figure 12. Electron Micrograph of Industrial Aluminum Surface Before Preparations.

Figure 13. Optical Micrograph of Sanded (Prepared) Aluminum Surface for Tensile Experiments. Circle Encloses the Area Illuminated by the Laser Beam.

Figure 14. Defects Due to Tensile on Aluminum Specimen Surface After 8.5% Plastic Extension. Photograph Taken on the Neck of the Specimen.

Figure 15. Defects on Bent Aluminum Surface After a 90° Bend and Flattening Operation.

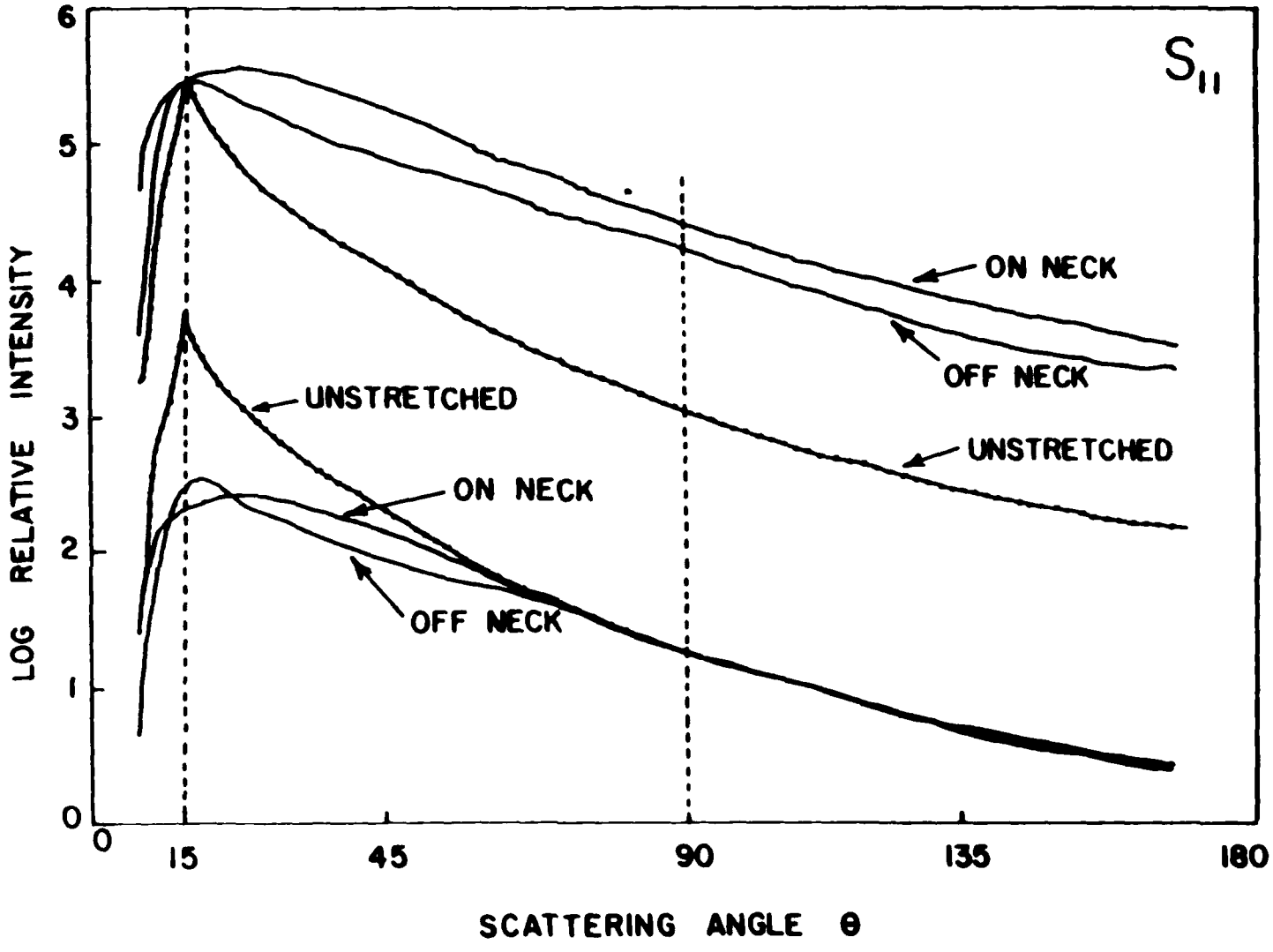

Figure 16 The S_{11} Matrix Element for the Tensile Specimen Before and After Extension ($\alpha = 7.5^{\circ}$). Top Set Normalized at $\theta = 15^{\circ}$, Bottom Set Normalized at $\theta = 90^{\circ}$.

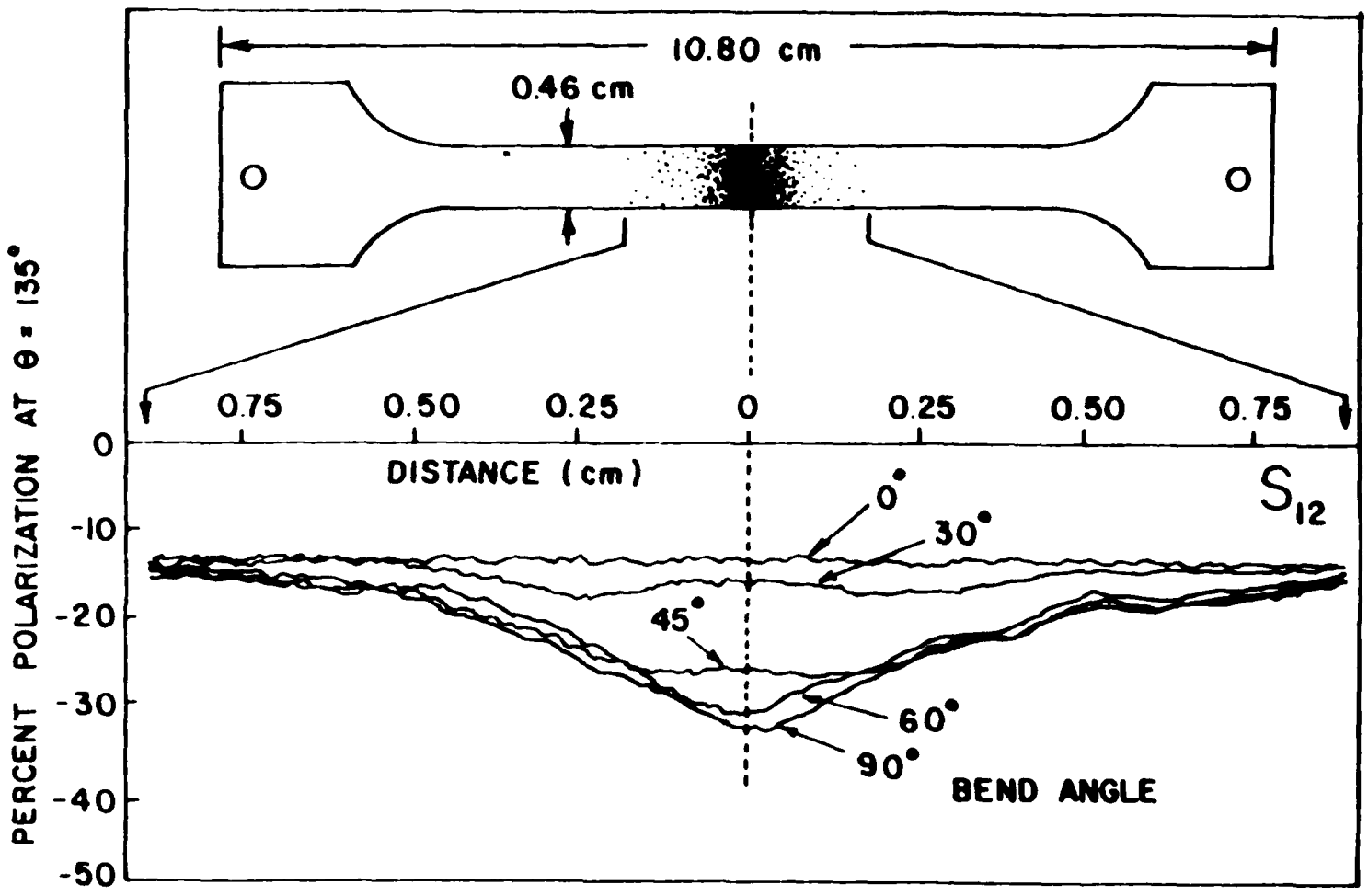

Figure 17. Top: A Drawing of the Aluminum Bend Specimen. The Dotted Area Represents the Bend Section. Bottom: The S_{12} Matrix Element at $\theta = 135^{\circ}$ as a Function of Position Along the Bend Specimen ($\alpha \sim 10^{\circ}$)

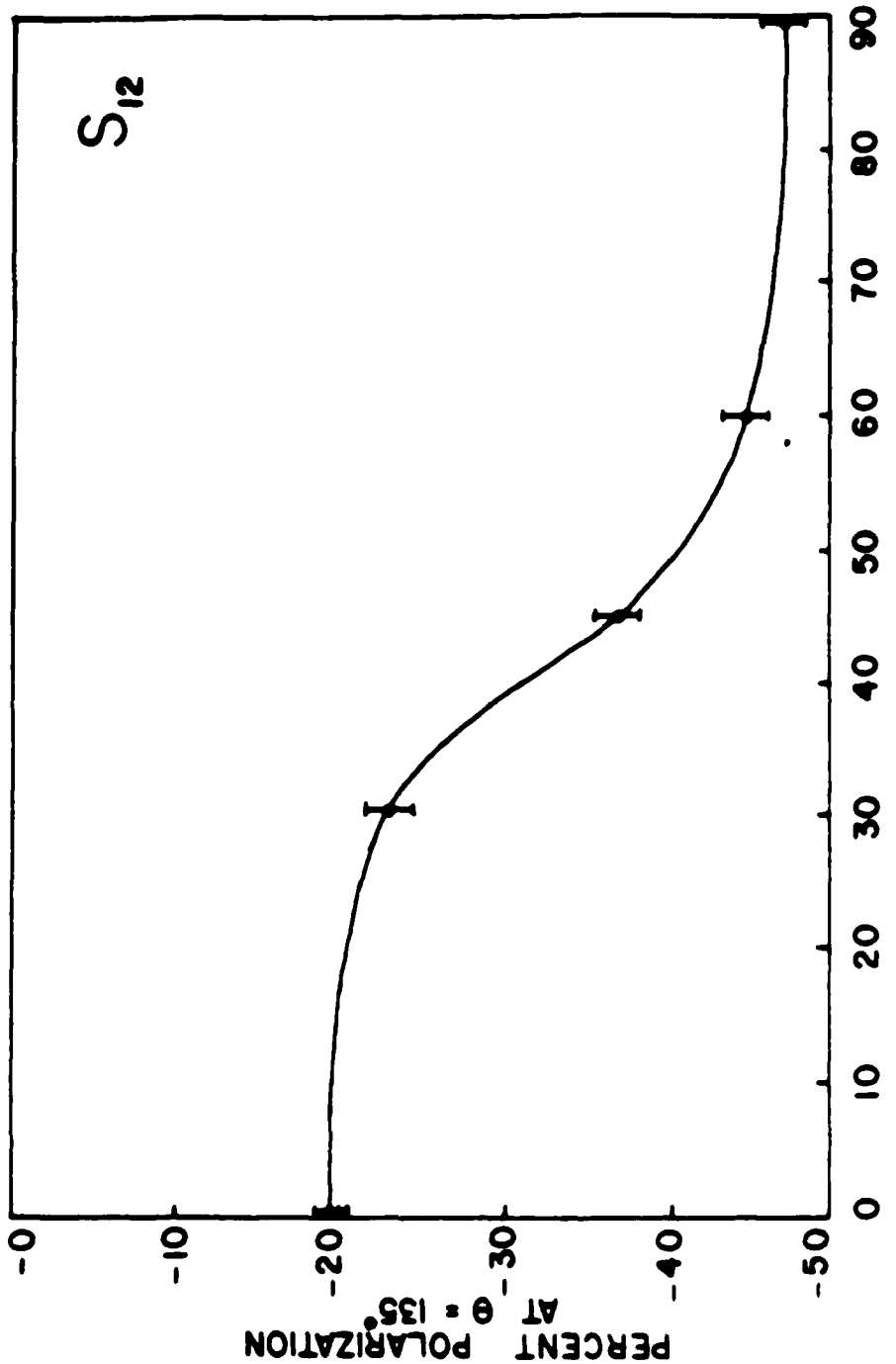

Figure 18 Response of the S_{12} Matrix Element at $\theta = 135^{\circ}$ as a Function of Bend Angle

matrix of the surface plus the line was measured as a function of the increasing size (height and width) of the line for various angles of illumination. The results are compared to scattering and diffraction data from a single slit and opaque circular cylinder of equal dimensions. The following figures 19 - 24 taken from this paper show the data and results of these experiments.

2.10) W. S. Bickel and G. Videen, "Loss of Oscillatory Phase Information on Light Scattering Curves," Aeresol Science and Tech, 1986 (Submitted)

The accuracy of information about scatterers extracted from light-scattering data depends on the amount of phase information on the light-scattering curves. Perfect monodispersed single spheres give the highest quality phase information from which all particle properties can be exactly and uniquely determined. When phase information is reduced or absent, much less can be learned about the scatterers. We examined in detail some important and common reasons for phase loss in light-scattering curves and comment in what information might still be extracted.

2.11) W. S. Bickel, G. Videen, and S. Tidwell, "Light Scattering as a Probe for Change," for Aeresol Science and Tech. (In Preparation)

This work shows how the S_{ij} respond one parameter change as all other optical and geometrical parameters are held constant. For small changes, any S_{ij} responds "linearly" as a particular parameter (say n_1) increases linearly. During this linear increase, a second parameter increases and decreases. This additional perterbation is detected by the S_{ij} and gives a measure of how effective masking is.

2.12) G. Videen and W. S. Bickel, "Light Scattering from MgO Coated Quartz Fibers," for App. Optics. (In Preparation)

Perfect cylindrical quartz fibers are increasingly coated with MgO crystals while S_{ij} are measured as a function of coating "thickness". Even when virtually all phase information is destroyed, the remaining signal can yield the approximate size of the coated fiber.

2.13) G. Videen, W. S. Bickel and D. Abromson, "Polarized Light Scattering from a Perfect Cylindrical Quartz Fiber on a Perfect Aluminum Surface." (In Preparation)

All 16 matrix elements are measured for the light scattered from cylindrical quartz fiber on a mirror surface. The results are compared to the fiber in air, and the surface with out the fiber. The near field interaction of the fiber surface geometry severely distorts all fiber matrix elements and makes identification of the "defect" essentially

Figure 19. SEM Micrograph of Sample L4 Magnified Seventeen Thousand Times. Bar line = 1 micron.

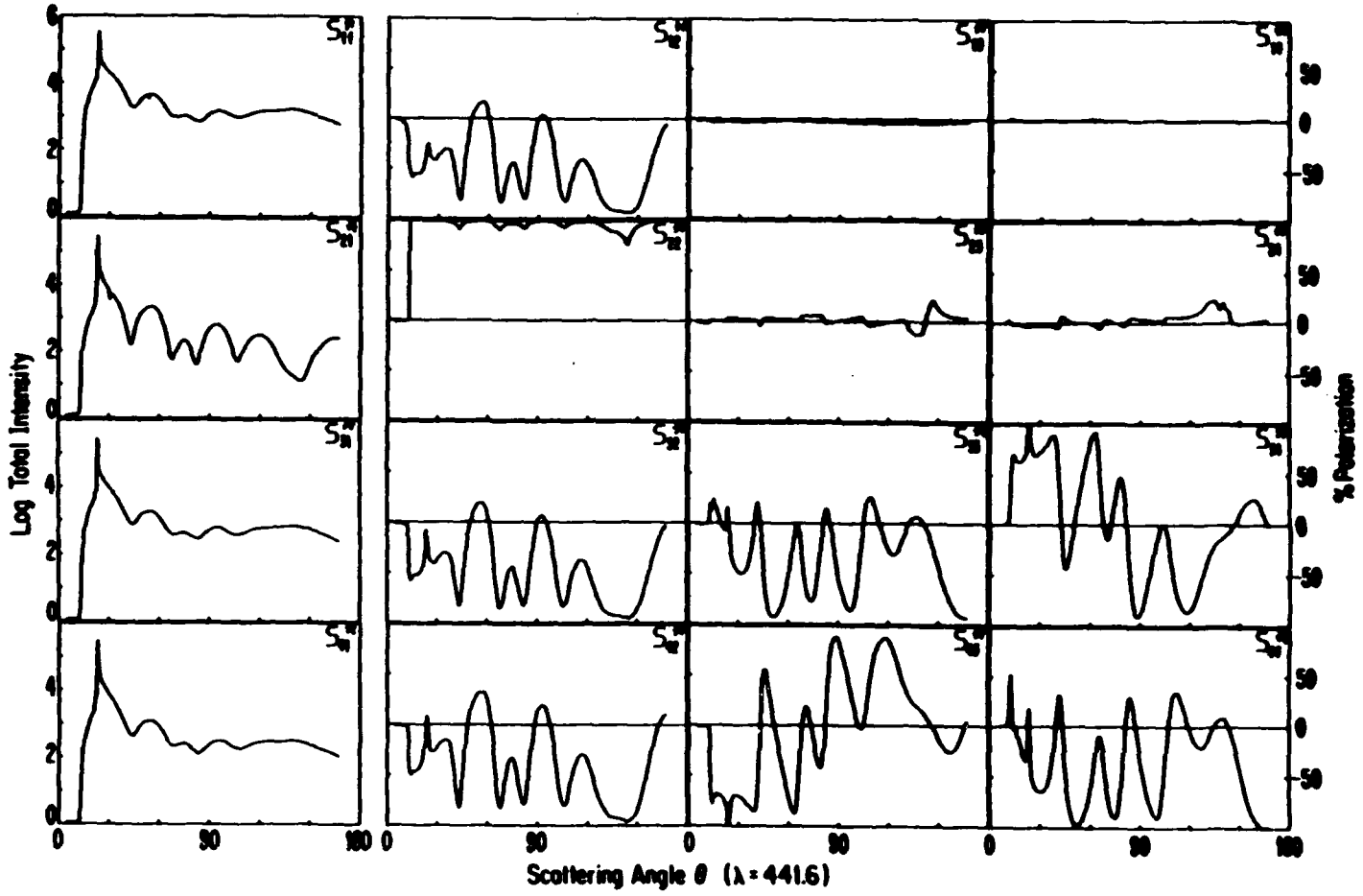

Figure 20. The Entire Mueller Matrix, S^*_{ij}, for Sample L4 Illuminated at Grazing Incidence ($\alpha = 11^\circ$).

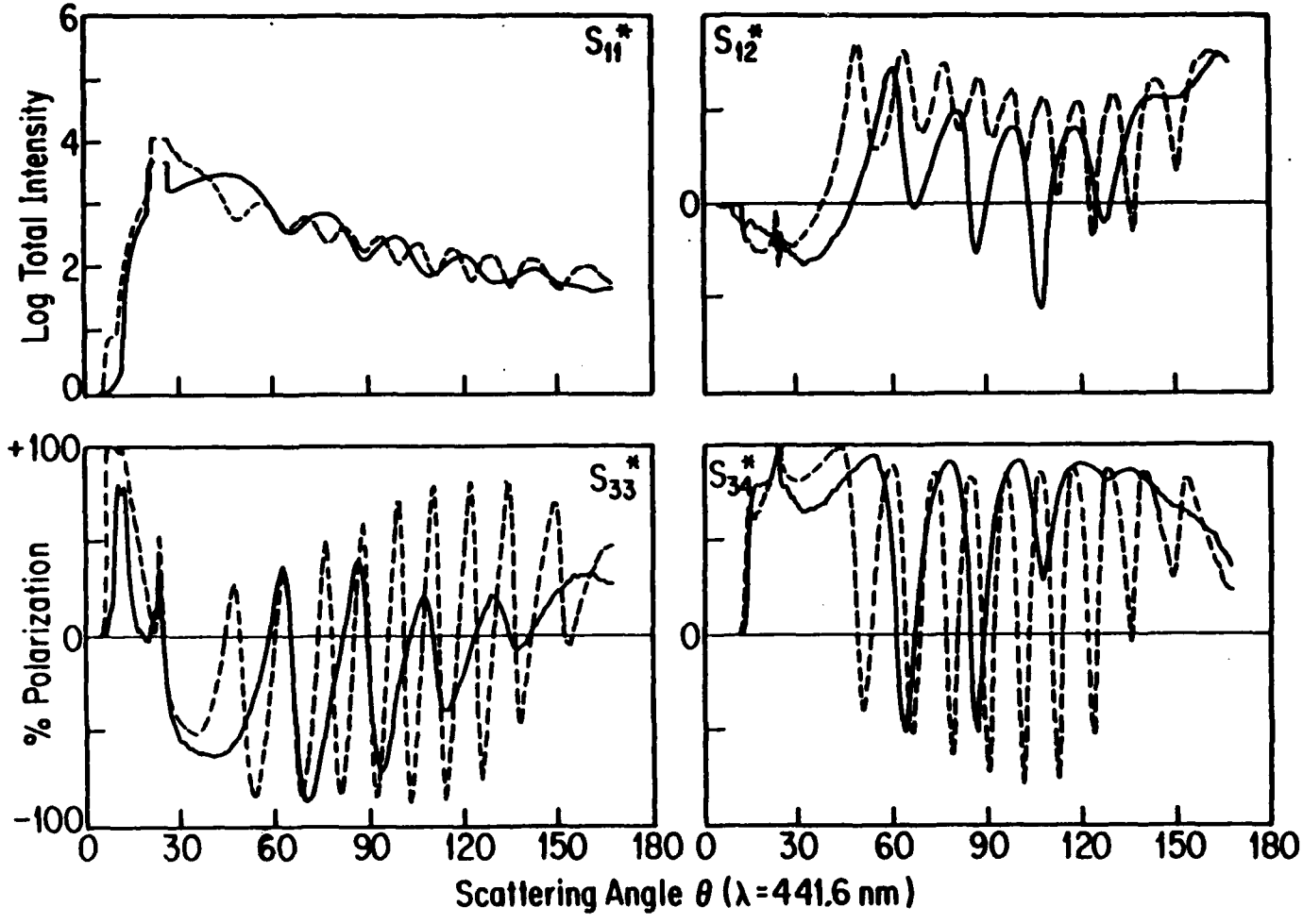

Figure 21. (Solid Line) The Matrix Element Curves for Sample L2 (height = 1000Å, width = 1.0 m) and (Dashed Line) Sample L2W (height = 1000Å, width = 2.3 m) Both at Grazing Incidence ($\alpha = 11^{\circ}$).

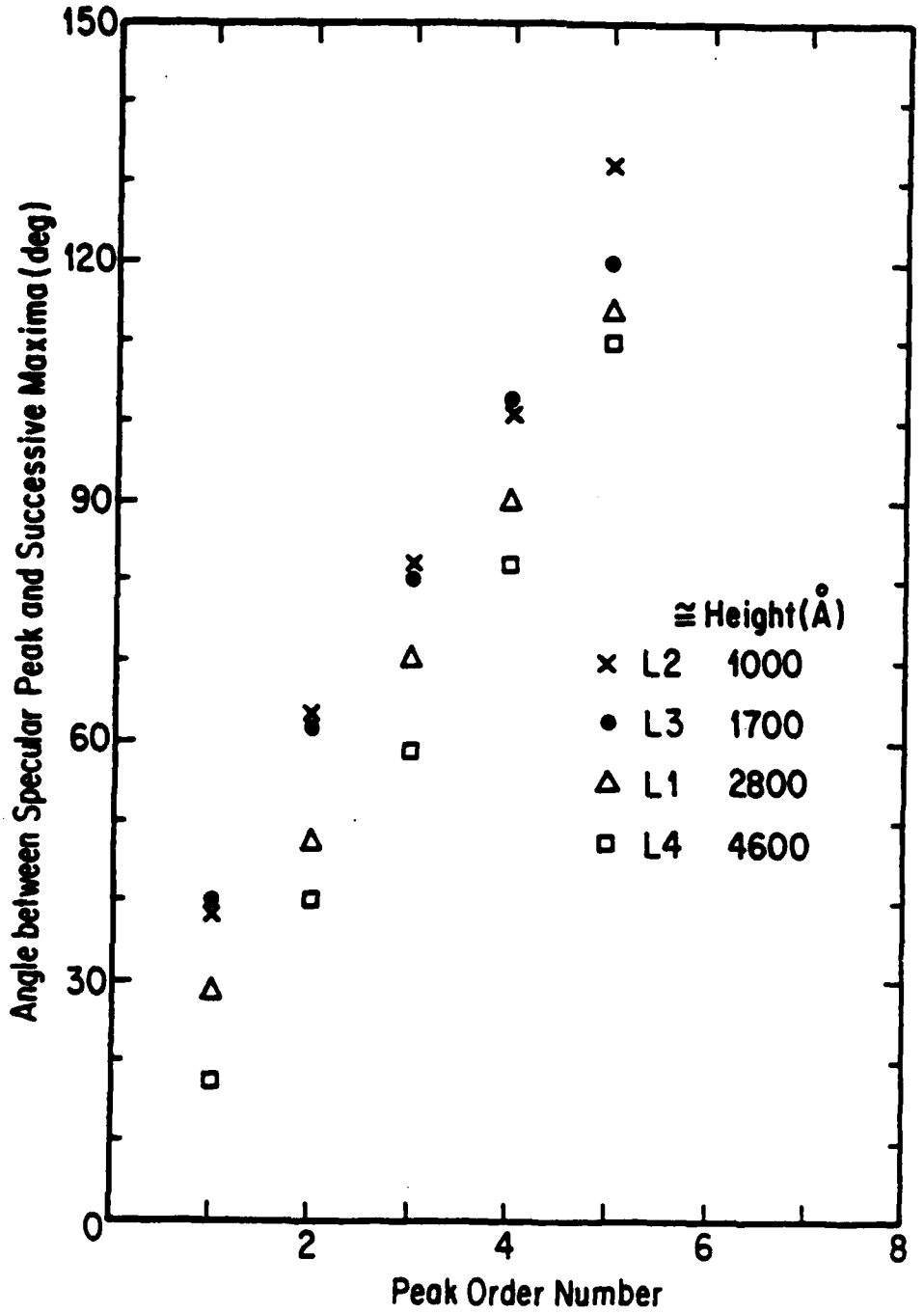

Figure 22. Rotational-Height Study Plots of the S_{33} Matrix Element Maxima at Grazing Incidence ($\alpha = 11^{\circ}$) for Samples L4, L1, L3 and L2. Note: Error bars are approximately the size of the data point characters.

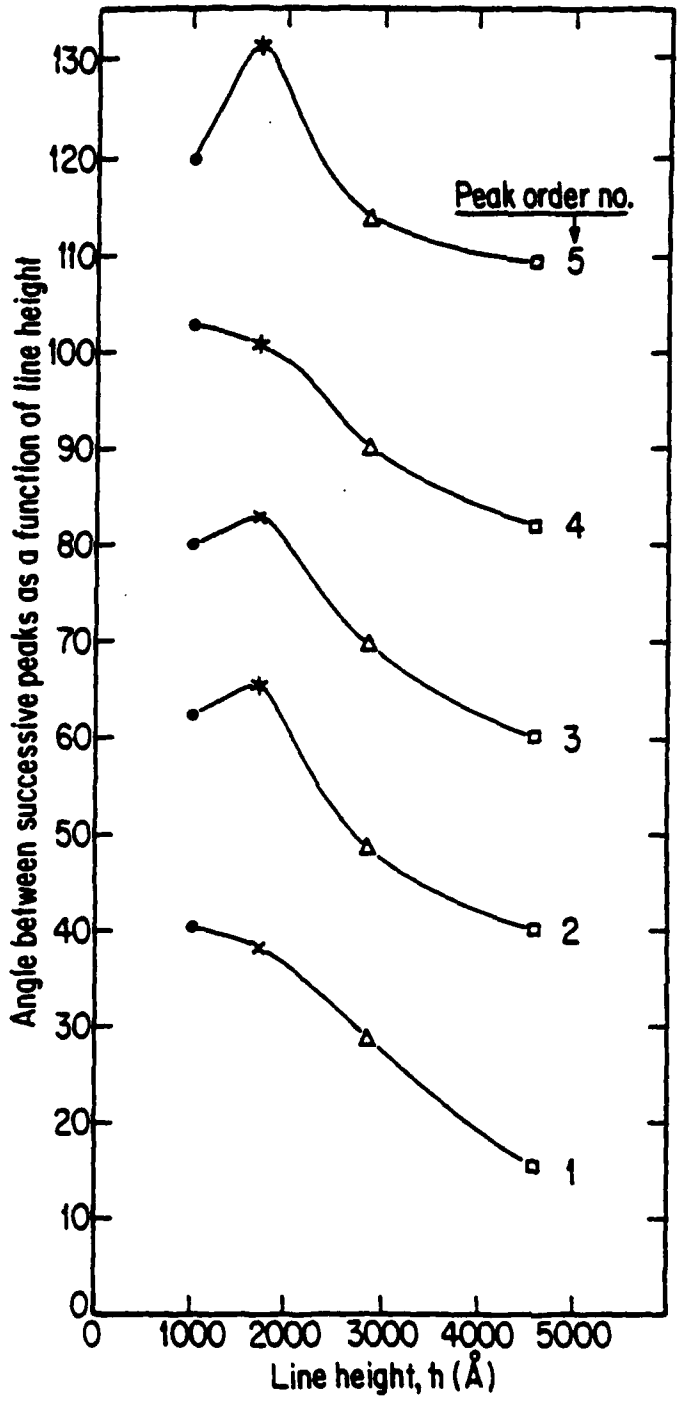

Figure 23. The Angle Between Successive Peaks as a Function of Line Height.

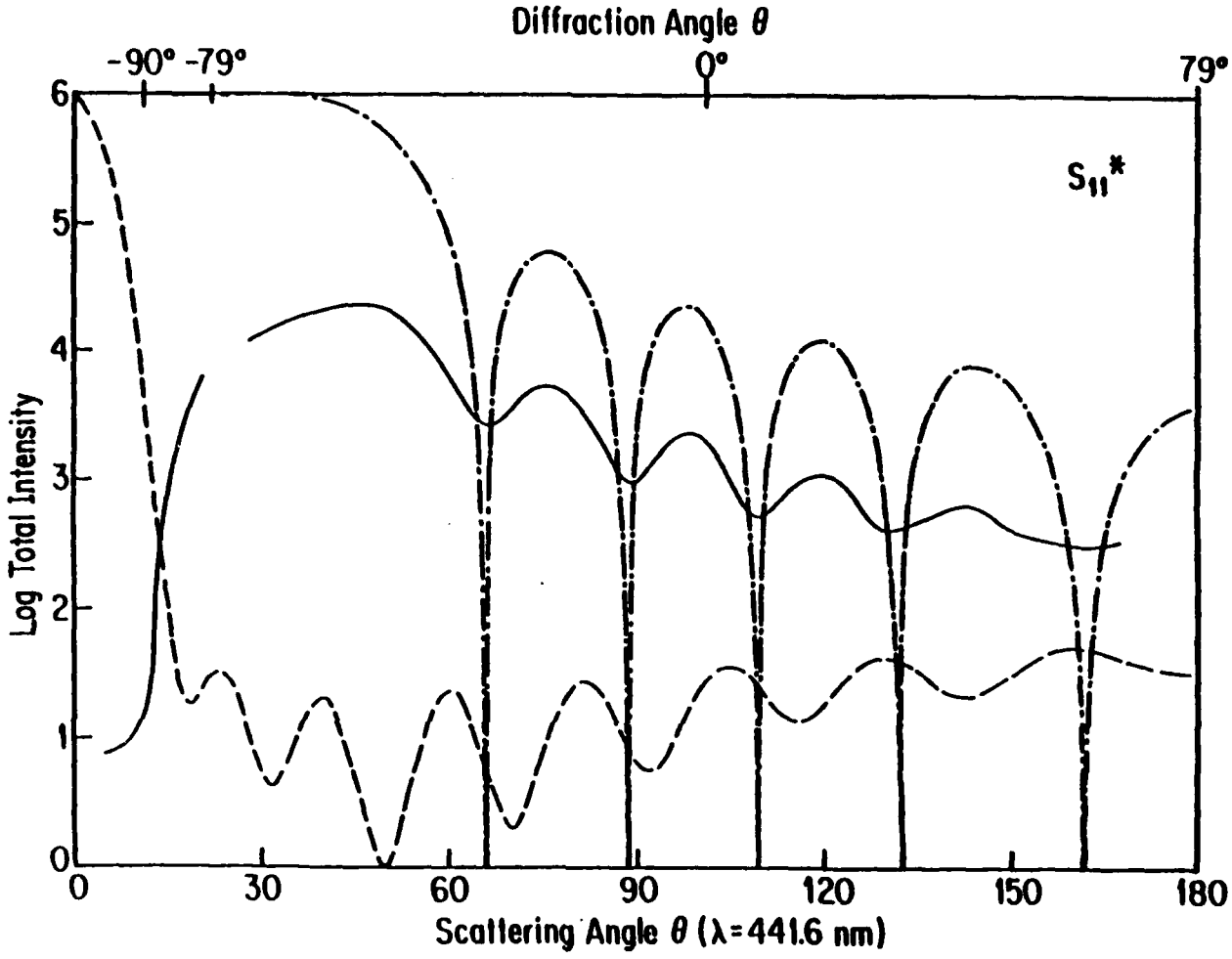

Figure 24. (———) The S_{11}, Total Scattered Intensity, Curve from Sample L2 (height = 1000A, width = 1.0m) Illuminated at Grazing Incidence ($\alpha = 11^{o}$). (The Specular Peak ($\Theta = 22^{o}$) has been omitted for convenience.) (-.-.-.-) The Theoretical Diffracted Intensity Distribution from a Single Slit (Slit Width = 1.2 m) Illuminated at Grazing Incidence ($\alpha = 11^{o}$). The Diffraction Angle $\Theta = 0^{o}$ Corresponds to the Direction of the Slit Normal. (----) The Theoretical Scattering S_{11} Curve for an Aluminum Cylinder (Diameter = 1.2 m).

impossible without prior knowledge of the scattering system.

2.14) D. Abromson and W. S. Bickel, "Fiber Extinction Measurements Using a Laser Ring Cavity," for JOSA. (In Preparation)

The detuning (perturbation) of a ring cavity by a small particle (fiber) gives information about the fiber size. The new cavity decay time with perturber inside gives the total extinction cross section for the particle.

2.15) W. S. Bickel and S. Tidwell, "Light Scattering from Two Types of Red Blood Cells," for J. Bio. Phys. (In Preparation)

The S_{34} and other matrix elements are evidently able to discriminate between certain blood types of human red blood cells. We also find that the actual signals are dependent on preparation techniques and of course impurities.

2.16) D. Abromson, "Small Particle Perturbation of a Laser Ring's Cavity Decay Lifetime," M.S. thesis, Physics Dept., Univ. of Arizona, 1986.

The measurement of a laser ring cavity's decay lifetime can provide information about a small particle's total extinction cross section. We used a perfect sub-wavelength and a near-wavelength diameter, quartz fiber to perturb a passive laser ring cavity. A plot of decay lifetime versus relative fiber displacement in the laser ring cavity showed the decay lifetime's dependence on the fiber's position with respect to the nodes of a standing electromagnetic field wave in the cavity and fiber's size compared to a wavelength. The fiber's radius was measured with a polar nephelometer. Then using each radius and Mie theory, the forward and backscattered values and the total scattering cross section were obtained for the two nonabsorbing quartz fibers. Finally, the total extinction for each fiber was calculated using the average decay lifetimes and the theoretical scattering values at 0° and 180°.

2.17) K. Nahm, "Light Scattering by Polystyrene Spheres on the Conducting Plane," Ph.D. dissertation, Physics Dept., Univ. of Arizona, 1985.

A system consisting of a sphere sitting on a clean mirror was modeled as a two particle system: the real sphere and its image sphere, treating the mirror as a conducting plane. When the system was irradiated with a plane-polarized collimated laser beam with varying angles of incidence, the scattering from each particle was assumed to follow Mie's solution for light scattering by a sphere. Phase difference between the scattering by the real sphere and the one by its

image sphere was assessed by the geometry of the model. The far field solutions from each of the spheres were added to yield a phase correlation between the two and the intensities from each spheres were added. Also discussed is the Double Interaction Mode, which takes the mirror-sphere separation into consideration. These theoretical results were converted to Bidirectional Reflectance Distribution Functions (BRDF). The theoretical as well as the empirical surface scattering from a good quality optical surface was introduced. The BRDF values thus calculated were added to the background scattering by the mirror since no interaction was assumed between the spheres and the rough metallic surface of the mirror. The test sample was prepared with polystyrene spheres with the nominal diameter of 0.984 m on a high quality aluminum mirror. The BRDF data from this sample with 6328A and 4416A were compared with the one obtained with the model described above. The comparison strongly indicated that there existed no phase correlation between the scatterings by the two spheres. Determination of the sphere size and practical applicability for estimating the sphere number density on the surface are also discussed.

2.18) V. Iafelice, "The Polarized Light Scattering of Matrix Elements for Select Perfect and Perturbed Surfaces," M.S. thesis, Physics Dept., Univ. of Arizona, 1985.

The angular distribution of scattered light is known to depend on the electromagnetic properties (index of refraction, absorptivity), the geometrical properties (size, shape, and distribution) of the scatterer(s) as well as on the nature of the incident light. The entire 16 element Mueller matrix has been experimentally determined for a nominally smooth reflecting optical surface of aluminum which was illuminated with = 441.6 nm light at various angles of incidence. Additionally, a small rectangular line (whose known dimensions are of the order of the incident light) has been constructed of the same material (Al), on a similar surface. The Mueller matrix of the surface plus the line was measured as a function of the increasing size (height and width) of the line for various angles of illumination, . The experimental procedure and results are discussed and compared with existing theories.

2.19) H. A. Yousif, "Light Scattering from Parallel Tilted Fibers," Ph.D. dissertation, Physics Dept., Univ. of Arizona, expected 1986.

The Mueller scattering matrix elements (S_{ij}) and the cross sections for the scattering of an electromagnetic plane wave from two infinitely long parallel circular cylinders at oblique incidence are derived. Each cylinder can be of different arbitrary materials, i.e. any refractive index. The incident wave can be in any polarization state.

To find the scattering coefficients, which are essential for calculating S_{ij} and the cross-sections, the multiple scatterings were taken into account for all orders such that the total field in the vicinity of one cylinder is the true incident field plus the scattered field from the other cylinder.

The solution of Maxwell's equations for this problem is expressed as a sum of Bessel functions, and the scattering coefficients are found by satisfying the boundary conditions.

A computer program is written. The scattering coefficients are calculated from a matrix equation.

This is the first comprehensive study of the two cylinder problem. Special cases are considered in comparison with other published works. Calculations are shown of S_{ij} and of cross-sections for some selected cases of configurations of the two cylinders. The following figures 25 - 36 taken from this thesis show some of the data resulting from this research.

2.20) W. S. Bickel and V. Iafelice, "Polarized Light Scattering from Surfaces," Proceedings of the 1985 CRDC Scientific Conference on Obscuration and Aerosol Research.

The 1985 ARMY CRDC report describes our approach to polarized light scattering studies of smooth and rough surfaces. We introduced the concept of surface masking and controlled coating to follow the surface from one equilibrium surface to another.

2.21) W. S. Bickel and V. Iafelice, "Polarized Light Scattering from Surfaces," Proceedings of the 1986 CRDC Scientific Conference on Obscuration and Aerosol Research.

This 1986 ARMY CRDC report describes our work with perfect surfaces, perturbations on perfect surfaces and liquid coated surfaces.

2.22) W. S. Bickel, V. Iafelice and G. Videen, "The Role of Polarization in the Measurement and Characterization of Scattering," SPIE 30th Annual International Technical Symposium on Optical and Optoelectronic Applied Sciences and Engineering, Aug. 1986.

When defects in optical elements scatter light they change its direction, intensity, and polarization. We discuss defect scattering in the context of the Stokes vectors and Mueller matrices that characterize the interaction.

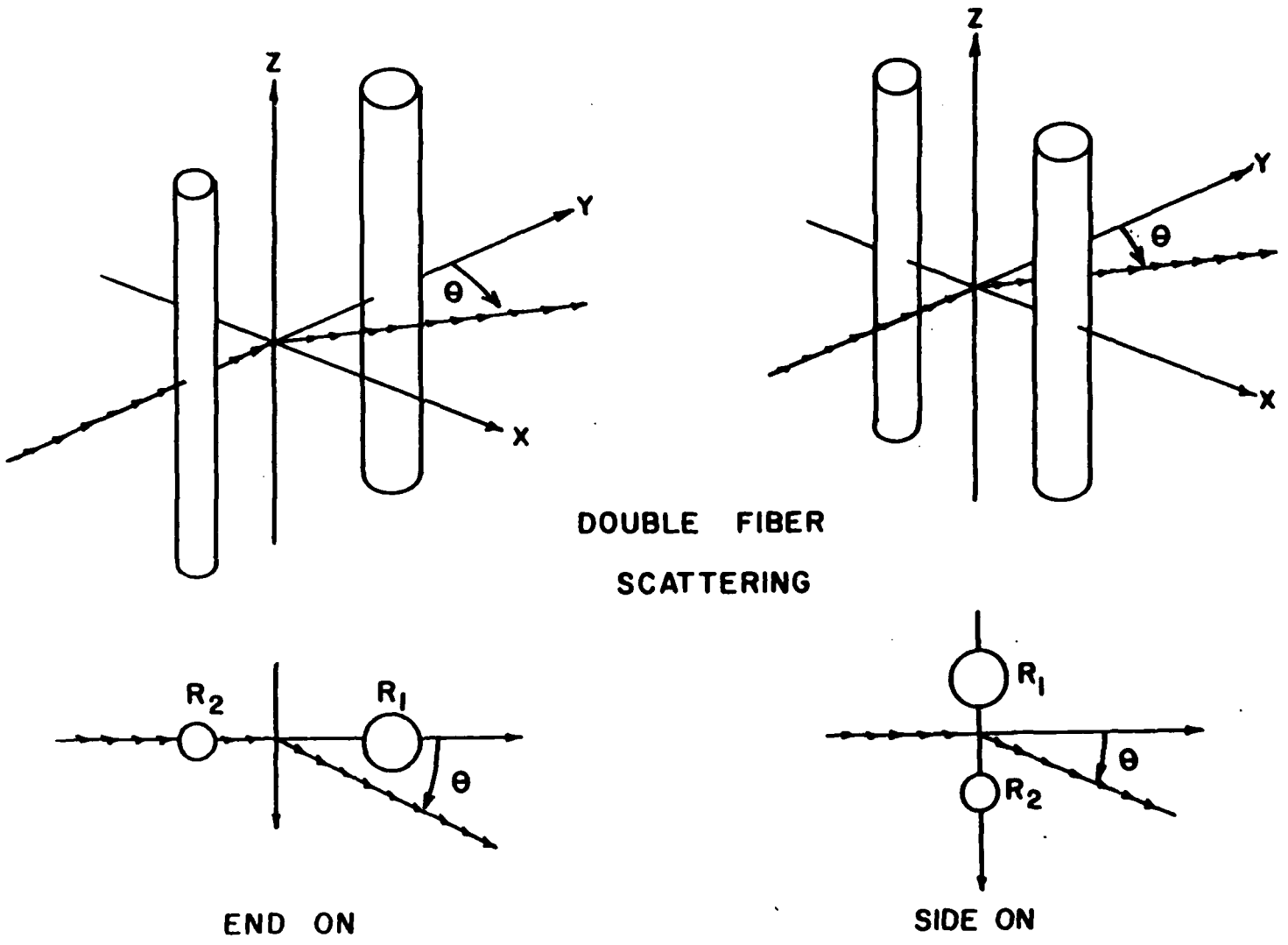

Figure 25. Geometrical Arrangement of Two Parallel Fibers and Laser Beam Showing End on and Side on Double Fiber Scattering.

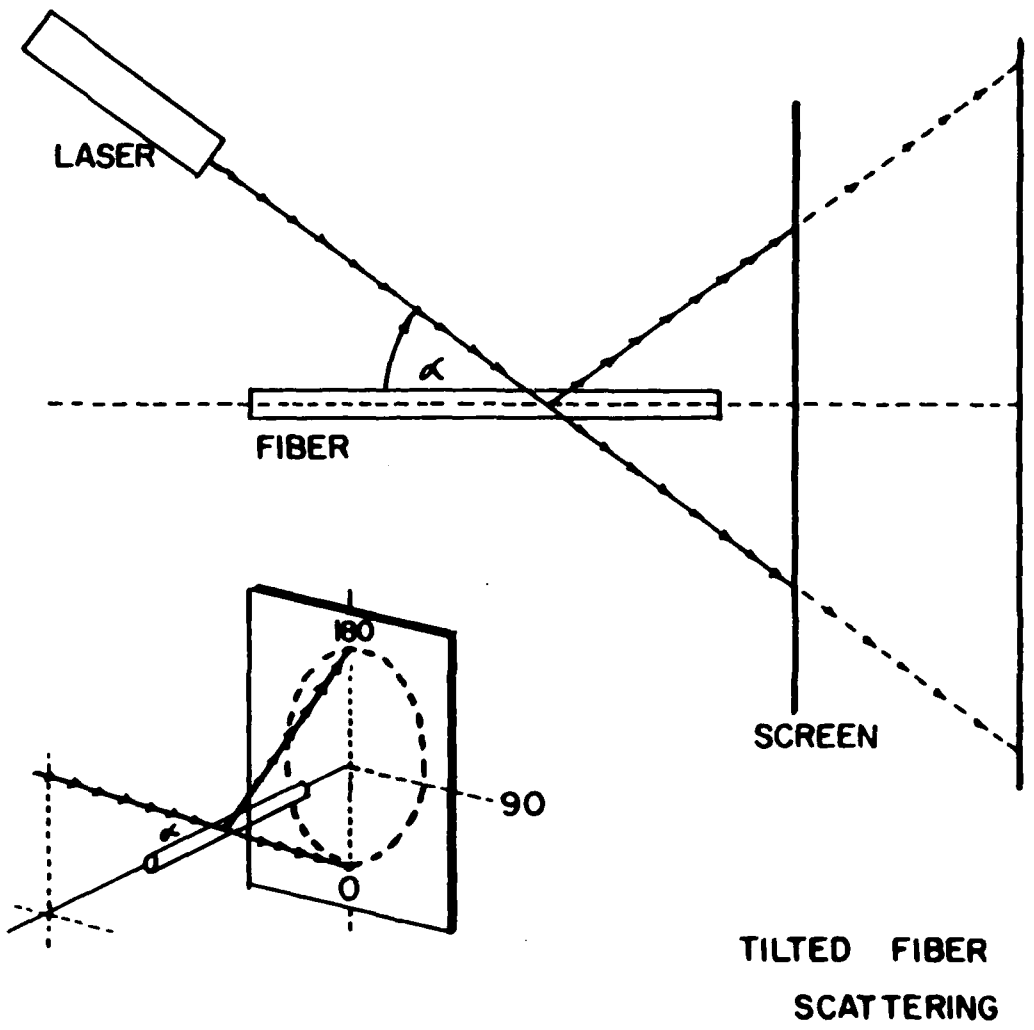

Figure 26. Geometrical Arrangement of Laser Beam and Detector Plane (Screen) for Tilted Fiber Scattering.

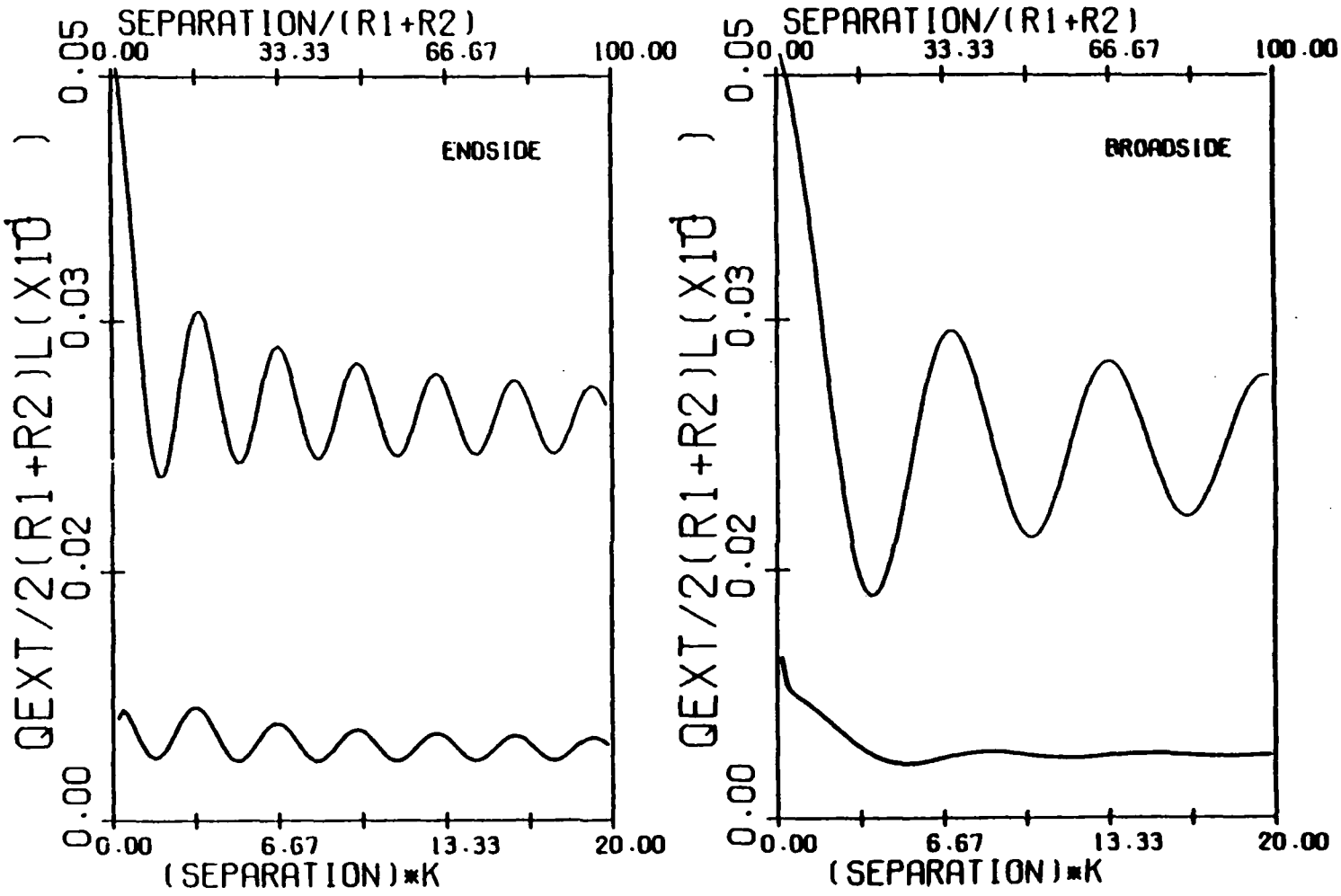

Figure 27. The Endside and Broadside Extinction Cross-Section as a Function of the Separation for the T.E. Polarization (Thick Line) and the T.M. Polarization (Thin Line).

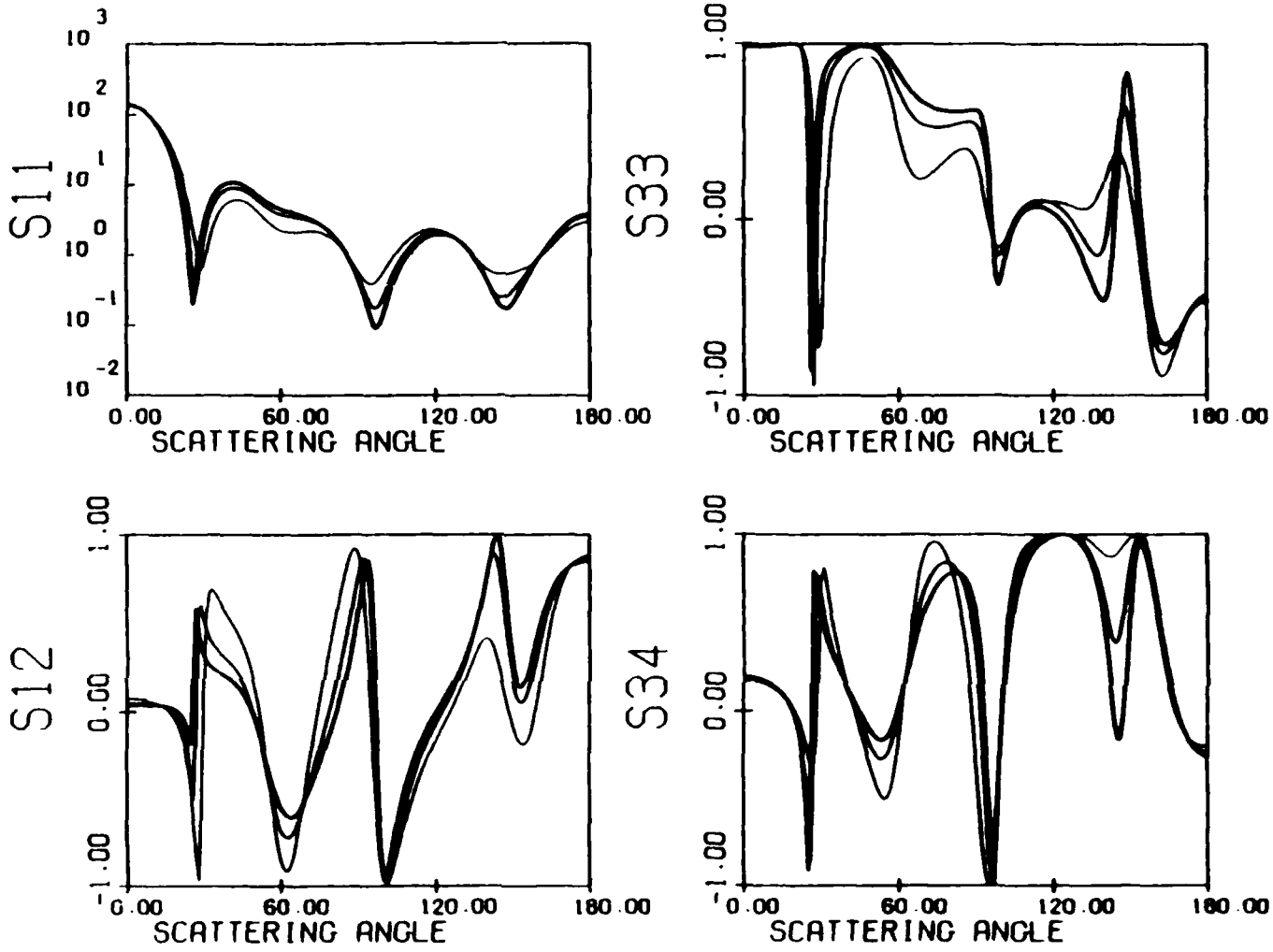

Figure 28. The Broadside S_{ij} as a Function of the Scattering Angle for Two Cylinders ($k_o a$ = 3.0, Refractive Index = 1.55, and λ = 0.6238 μ). The Thin Line is for Two Touching Cylinders, the Thick is for Two Cylinders Separated by 1.1 (R_1 + R_2) and the Thicker is for Two Cylinders Separated by 1.15 (R_1 + R_2

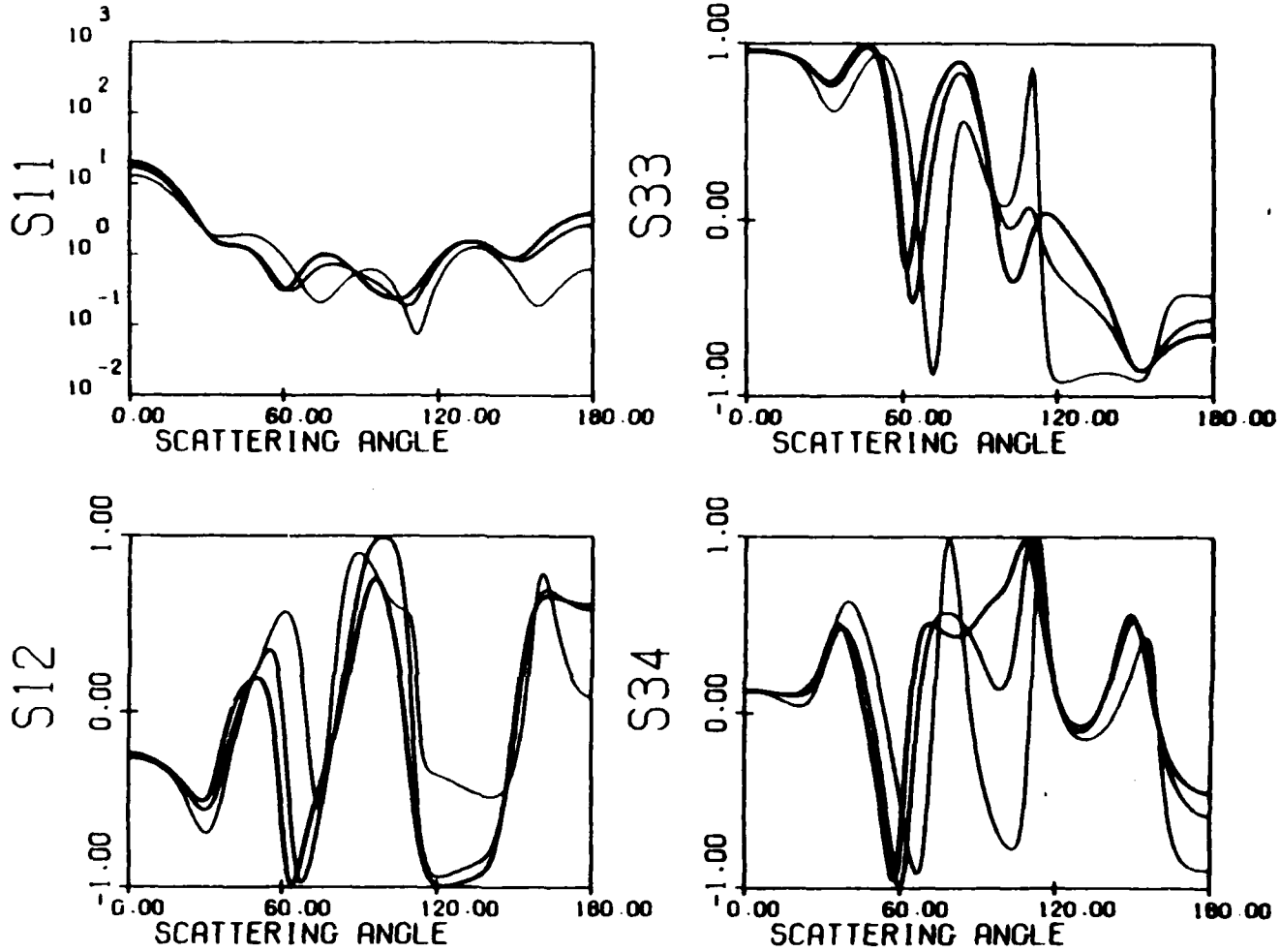

Figure 29. The Endside S_{ij} as a Function of the Scattering Angle for Two Cylinders ($k_o a$ = 3.0, the Refractive Index = 1.55, and λ = 0.6328μ). The Thin Line is for Two Touching Cylinders, the Thick is for Two Cylinders separated by 1.1 (R_1 + R_2) and the Thicker is for Two Cylinders Separated by 1.15 (R_1 + R_2).

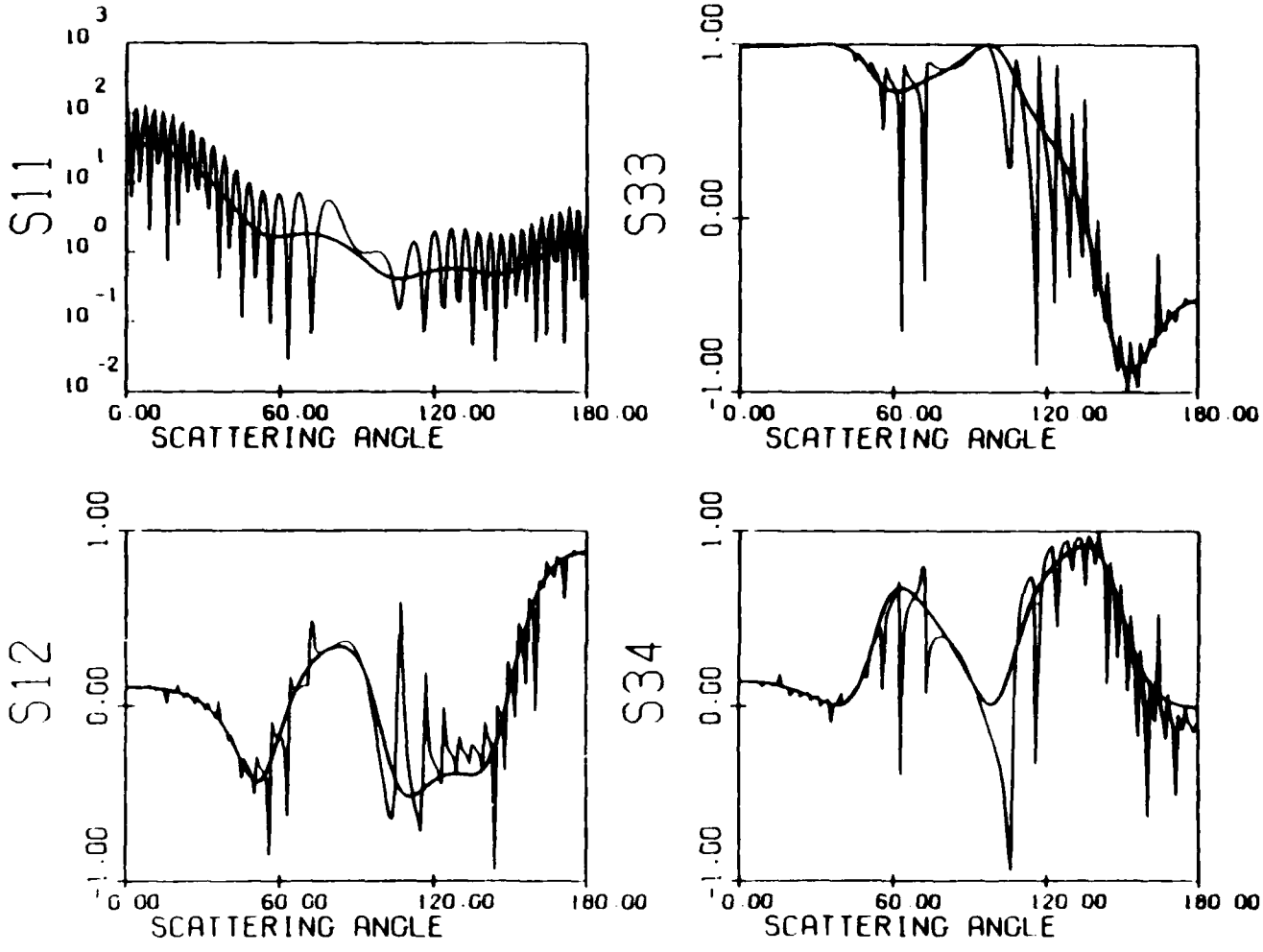

Figure 30 The Broadside S_{ij} as a Function of the Scattering Angle for a Single Cylinder (Thick Line) and Double Cylinders Separated by 17 $(R_1 + R_2)$ The Size Parameter of Each is 5.0 and Refractive Index = 1.55 The Wavelength of the Incident Wave is λ

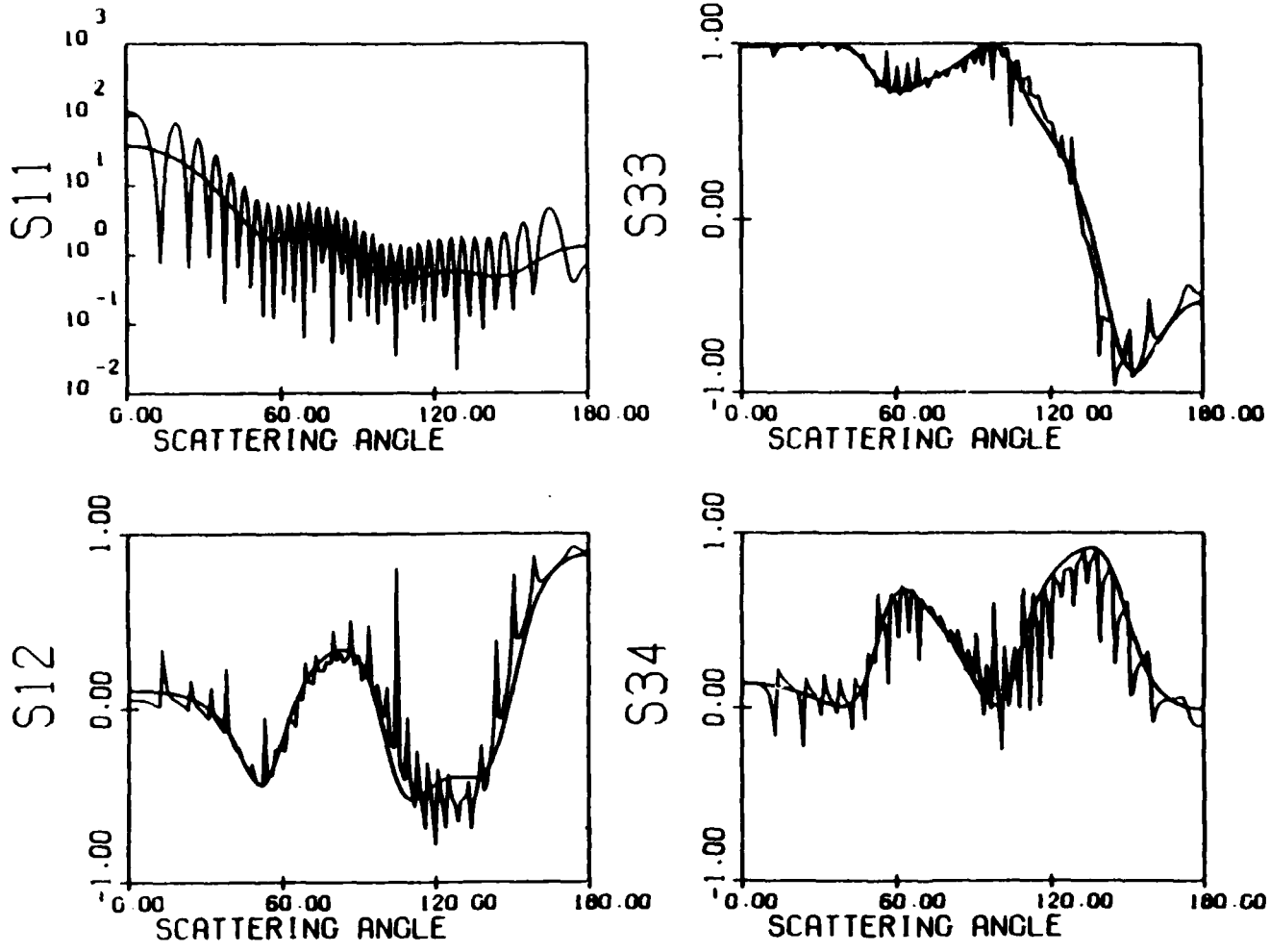

Figure 31. The Endside S_{ij} as a Function of the Scattering Angle for a Single Cylinder (Thick Line) and Double Cylinders Separated by 17 (R_1 + R_2). The Size Parameter of Each is 3.0 and Refractive Index = 1.55. The Wavelength of the Incident Wave is 0.6328μ.

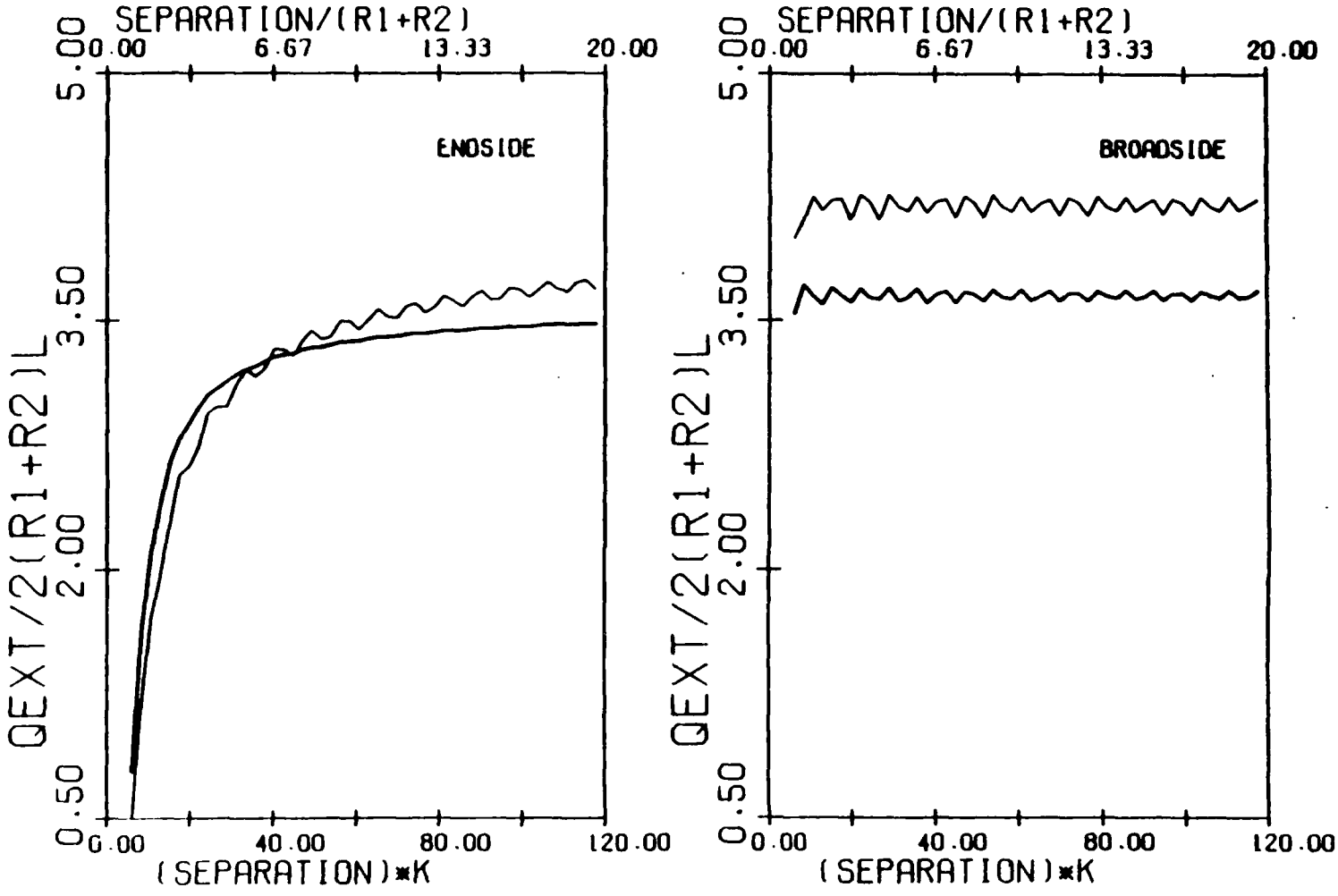

Figure 32 The Cross-Section per Unit Area for Two Dielectric Cylinders ($k_o a = 3.0$, Refractive Index = 1.55, λ = 0.6328μ) as a Function of the Separation ($k_o d$) of Normal Incidence

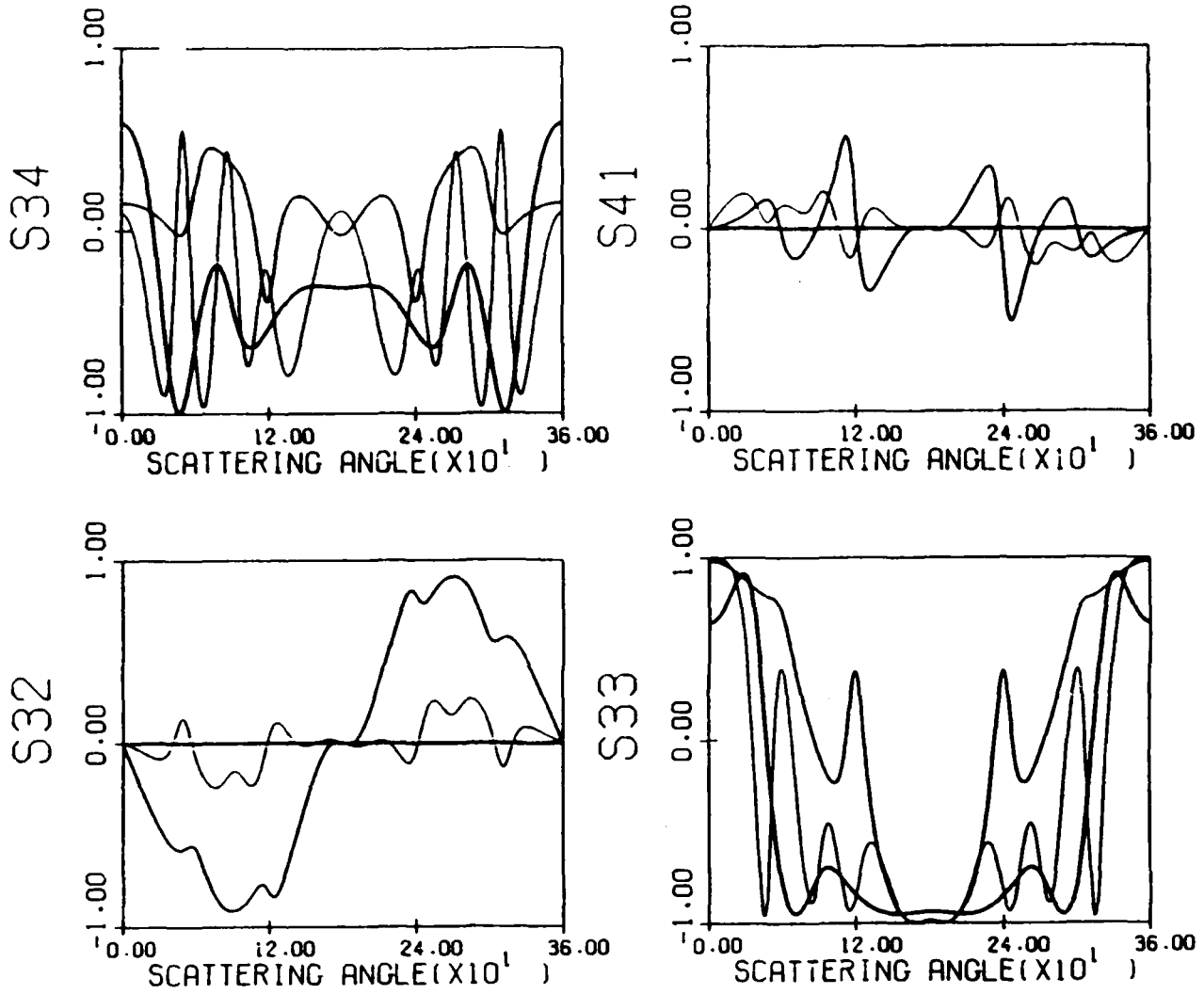

Figure 33. The Endside S_{ij} as a Function of the Scattering Angle for a Perfectly Conducting (Thick) and Dielectric Single Cylinder (Thin Line) and Both Cylinders Separated By 1.15 (R_1 + R_2) (Thinner Line). The Tilt Angle is 60°

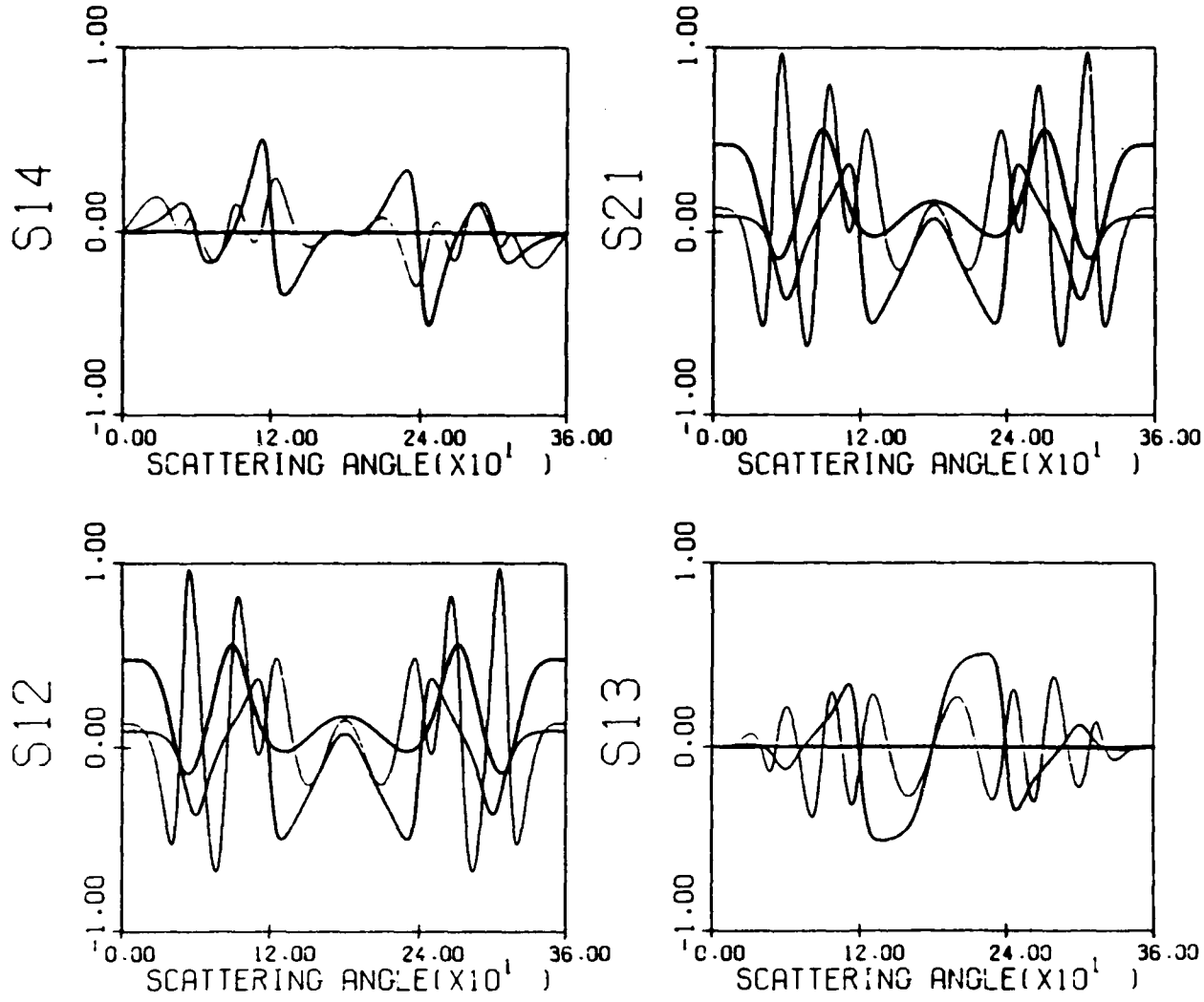

Figure 34. The Endside S_{ij} as a Function of the Scattering Angle for a Perfectly Conducting (Thick) and Dielectric Single Cylinder (Thin Line) and Both Cylinders Separated by 1.15 (R_1 + R_2) (Thinner Line). The Tilt Angle is 90°

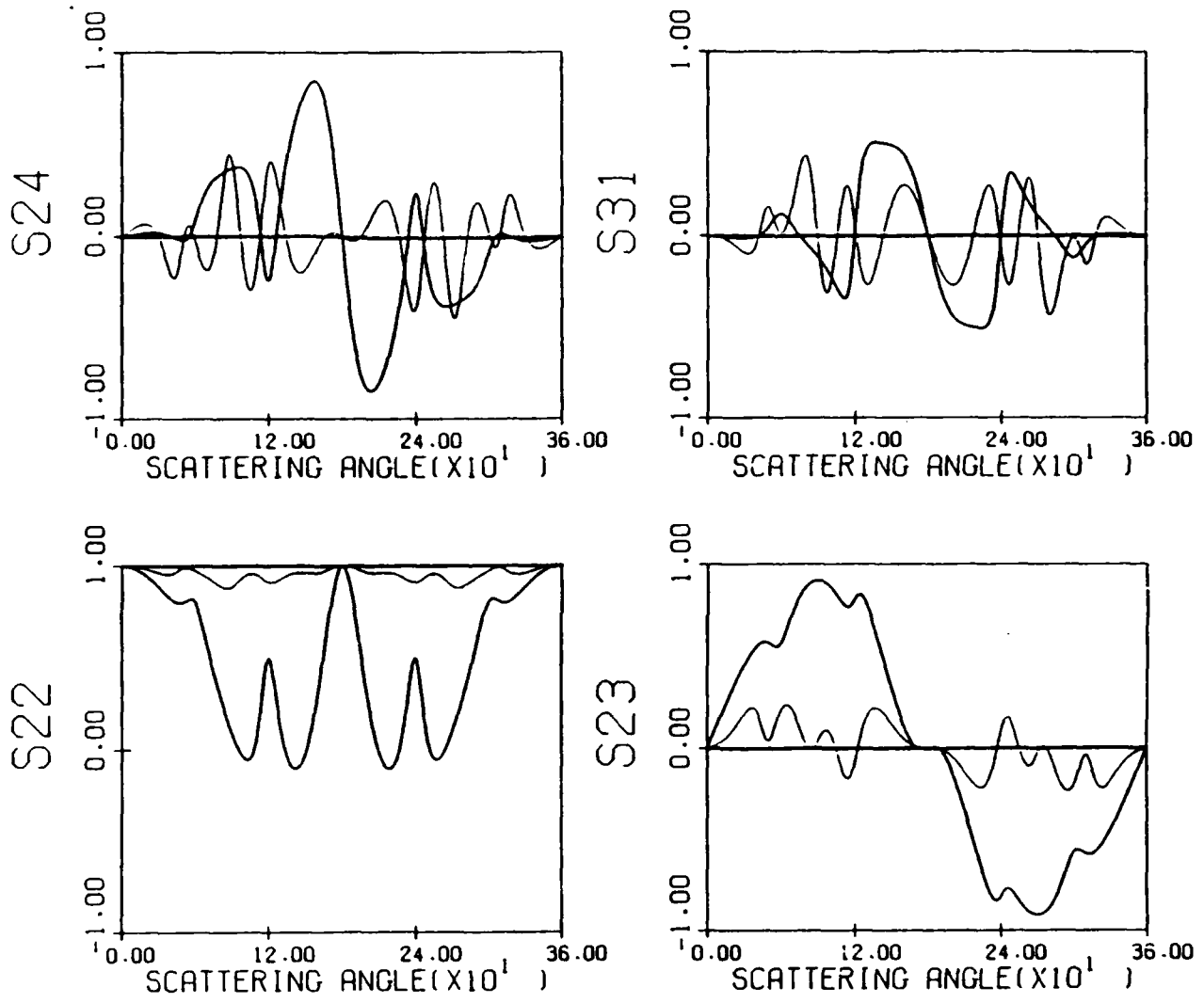

Figure 35. The Endside S_{ij} as a Function of the Scattering Angle for a Perfectly Conducting (Thick) and Dielectric Single Cylinder (Thin Line) and Both Cylinders Separated by 1.15 (R_1 + R_2) (Thinner Line). The Tilt Angle is 60°.

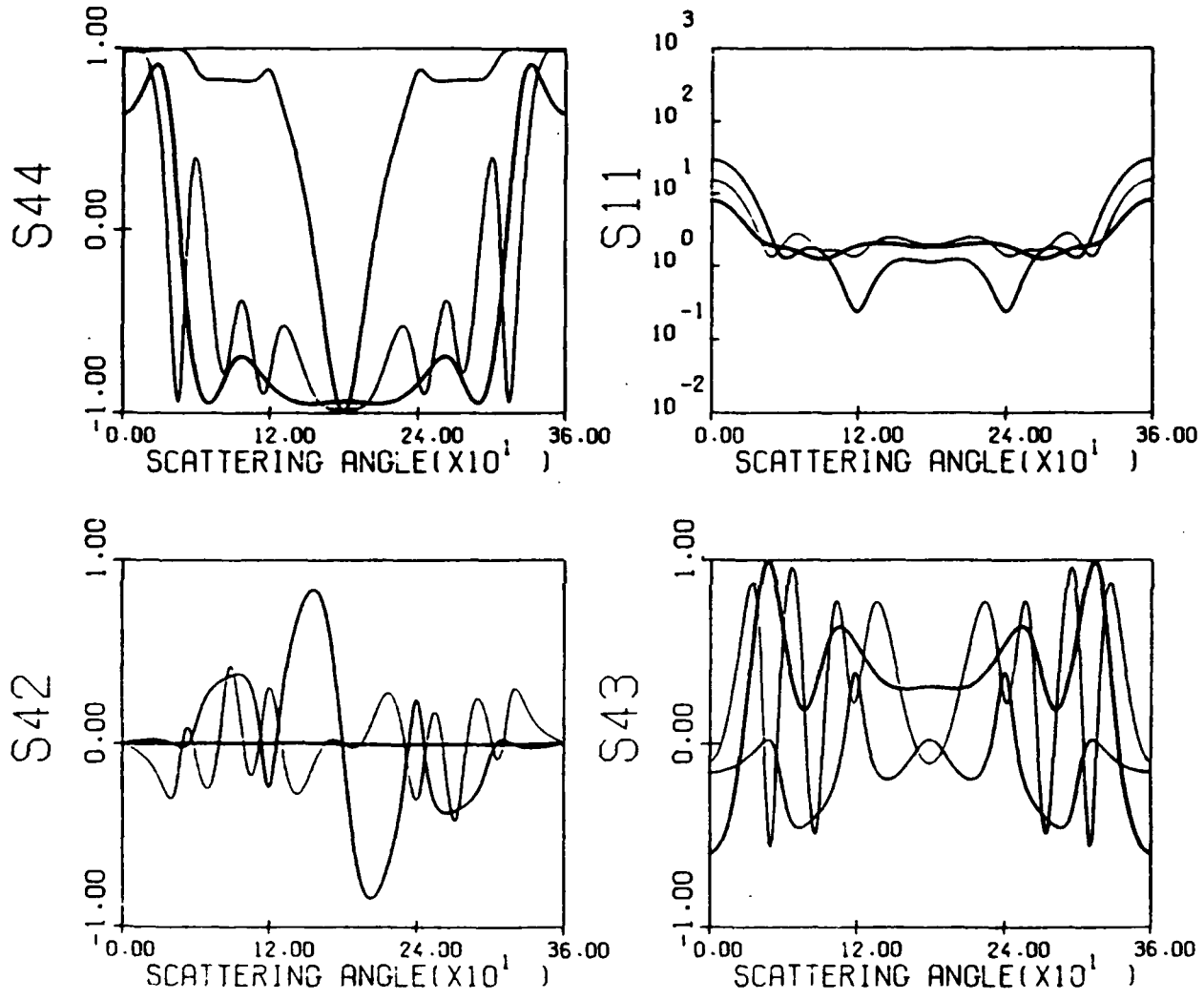

Figure 36. The Endside S_{ij} as a Function of the Scattering Angle for a Perfectly Conducting (Thick) and Dielectric Single Cylinder (Thin Line) and Both Cylinders Separated by λ ($R_1 + R_2$) (Thinner Line). The Tilt Angle is 60°.

2.23) W. S. Bickel "Polarized Light Scattering from Select Surfaces," Technical Report Submitted to US Army Chemical Research and Development Command, Dec. 1985.

Light scattering studies of five surfaces were made as a function of surface coatings with two different kinds of oils. The results show that the matrix elements signals are characterizers of the different surfaces and are sensitive to the kind of coatings and coating thickness.

Matrix element S_{11} shows trends in the forward-backscatter ratio, the amount of 90 degree scatter and in the scatter-reflectance ratio. S_{12} shows shifts in the angle of maximum polarization and zero crossing points. S_{33} always has at least one crossing point which seems to be a function of coating type and thickness. S_{34} signals are essentially insensitive.

We also studied the flouresence of the "light oil" illuminated with ultraviolet light (= 2537A) from a mercury lamp and with the 4416 A radiation line from the He-Cd laser. Strong flouresence occurs at the higher wavelengths in both cases. The flourescent region spans a 2000 A region reaching its maximum intensity at 3500 A. This flouresence can be used to detect the presence of the oil if its wavelength spectra is specific to the oil.

3. CONCLUSIONS

The experimental work carried out over the past two years with Army support is finished, and the major results have been reported in this final report. As with any good research, new questions have been asked and other paths of investigation have opened up. Therefore, the techniques we developed and the results we report will affect our ongoing research program for years with Army funding. Some other researcher will be supported by other grants.

A number of papers are in preparation for publication in the refered journals. Several topics reported in the results will be written as separate papers. We call special attention to the papers 2.8, 2.9, 2.13, 2.17, 2.18, and 2.19 which are the results of MS. and Ph.D research done with ARMY support. These papers report very high quality experimental data (from systems that have yet to be treated theoretically) and new theoretical data for double and tilted fibers (that have to be checked experimentally). In addition to the progress reports, and this final report, many results have been reported at seminars and colloquia in various departments throughout the University--chemistry, optical sciences, lunar and planetary sciences, geosciences, microbiology, etc.--wherever light scattering techniques are used to extract data. Researchers in those departments have benefitted greatly from our work on complex

particles, since most of their scatterers are irregular. The techniques developed in these experiments are now being applied to coated surfaces under an Army grant from CRDEC. It is interesting to see how these ideas were developed and extended from a sphere = point; to a fiber = line; to a surface = area. We are optimistic that the Mueller Matrix-Stokes Vector approach to light scattered from surfaces will also be a valuable contribution to fundamental science and technology.

END

9-87

DTIC